Early to mid-Holocene spatiotemporal vegetation changes and tsunami impact in a paradigmatic coastal transitional system (Doñana National Park, southwestern Europe)

Saúl Manzano[a], José S. Carrión[a], Lourdes López-Merino[b], Juan Ochando[a], Manuel Munuera[a], Santiago Fernández[a], Penélope González-Sampériz[c]

[a] Department of Plant Biology, Faculty of Biology, University of Murcia, 30100 Murcia, Spain

[b] Institute of Environment, Health and Societies, Brunel University London, Uxbridge UB8 3PH, UK

[c] Instituto Pireanico de Ecología, CSIC, Av. Montañana 1005, 50059, Zaragoza, Spain

Highlights

- Early to Mid-Holocene palaeoecological reconstruction from Doñana (SW Europe)
- Biotic and abiotic proxies reconstruct upland and aquatic vegetation systems.
- Upland stability contrasts with marshland elasticity in Doñana transitional systems.
- Groundwater-mediated terrestrial-estuarine connectivity is suggested.
- High-energy events triggered varying trajectories and tempos in vegetation dynamics.

Abstract

The southern European Doñana wetlands host a highly biodiverse landscape mosaic of complex transitional ecosystems. It is one of the largest protected natural sites in Europe, nowadays endangered by intensive agricultural practices, and more recently tourism and human-induced fires. Its present-day spatial heterogeneity has been deeply investigated for the last three decades. However, a long-term perspective has not been applied systematically to this unique landscape. In this new study, a palaeoecological approach was selected in order to unravel patterns of landscape dynamism comparing dry upland and aquatic ecosystems. A 709 cm-long sediment core was retrieved and a multi-proxy approach applied (palynological, microcharcoal, grain size, magnetic susceptibility, loss-on-ignition and multivariate statistical analyses). Pollen signatures show how sensitive aquatic wetland vegetation was to environmental changes while terrestrial vegetation was stable at millennial scale. The impact of several high energy events punctuates the Early and Middle Holocene sequence, two of which relate to the local tsunami record (~6.6 and ~9.1 cal. kyr BP). Contrasting impacts of these two events in the aquatic and upland ecosystems show the importance of landscape configuration and the contingent history as key elements for coastal protection.

Keywords

Holocene Transitional systems; High-energy events; Vegetation dynamics; Estuary; Tsunami; Refuge; Resilience; Biogeography; Aquatic plants

1. Introduction

Transitional systems such as coastal wetlands are amongst the Earth's most diverse and productive ecosystems (Newton et al., 2012, 2014). They play a significant role in carbon sequestration (Barbier et al., 2011), and provide numerous ecosystem services to humans, such as provisioning (e.g. raw material supply), regulation (e.g. biogeochemical cycling, water purification) and coastal protection services. Furthermore, coastal wetlands also attenuate erosion and the impact of waves and extreme climatic hazards on the coastline (Barbier et al., 2011). However, coastal areas are amongst the world's most populated areas and they concentrate increasing human pressures, threatening their diverse and unique ecosystems (Newton et al., 2012). In addition, understanding the role of transitional systems as buffers of extreme wave events (storms and tsunamis) is of interest for the inhabitants of coastal areas. Deep knowledge of coastal wetlands is thus, of hallmark importance. Certainly, the management of coastal wetlands can only be effective considering the interactions between the physical environment and the biological communities.

A paradigmatic case of transitional system in the westernmost part of Europe is Doñana, located in the mouth of the Guadalquivir (Southwestern Spain). This region, exhibiting a variable geomorphology (Rodríguez Ramírez, 1997), and large floristic (García Murillo et al., 2014, López Albacete, 2009, Rivas Martínez et al., 1980) and faunal (Díaz-Paniagua et al., 2015) richness, is protected under the Doñana National Park (DNP) ever since 1969. It is also an UNESCO biosphere reserve, an UNESCO World Heritage, and a Ramsar Wetland Site (Sousa et al., 2009). Hallmark in the DNP are the Guadalquivir River marshlands, amongst the biggest and most significant European wetlands, due to their seasonal character, high plant diversity, and their role as route for Palaearctic avian migrations (Martí and del Moral, 2002, Rendón et al., 2008).

Despite the ecological importance of the DNP, its long-term environmental history is poorly known. The great extension, complexity and heterogeneity of the Guadalquivir's marshlands, the secular history of human intervention, and the difficulty of recovering and contextualising environmental archives complicate completing palaeoecological studies (Lario et al., 2010a). While a considerable amount of research addressing the Quaternary geomorphological evolution of the mouth of the Guadalquivir is available (Rodríguez Ramírez, 1997, Rodríguez-Ramírez et al., 1997, Rodríguez-Ramírez and Yáñez-Camacho, 2008, and references therein; Ruiz et al., 2002, 2010), studies

on vegetation and landscape history are scanty and fragmentary (Jiménez-Moreno et al., 2015, Morales-Molino et al., 2011, Yáñez et al., 2006, Yll et al., 2003). This hinders our understanding of the extant terrestrial and aquatic biodiversity, the biogeographical patterns, and the autochthonous status of key species.

The overarching aim of this study is to fill these knowledge gaps by providing a new palaeoenvironmental reconstruction of the landscape heterogeneity and the infilling history of the mouth of the Guadalquivir transitional systems. The specific objectives are i) to reconstruct the aquatic vegetation history, disentangling the factors controlling long-term changes in aquatic assemblages along the infilling of the Guadalquivir palaeoestuary, ii) to reconstruct the Doñana upland vegetation history, discussing the mechanisms influencing community assemblages and the terrestrial-estuarine connectivity, and iii) to evaluate the impact of marine extreme wave events on the Guadalquivir area.

2. Material and methods

2.1. Study site

The DNP is located close to the mouth of the Guadalquivir River, in the southwestern part of the Iberian Peninsula (Fig. 1). The park comprises an extensive marshland of 140,000 ha. The marshland borders to the west with an aeolian dune field and it is isolated from the Atlantic Ocean by a mobile dune complex and a spit barrier (Rodríguez Ramírez, 1997) (Fig. 1b). The marshland is the result of the progressive Late Quaternary infilling of the Guadalquivir palaeoestuary (Rodríguez Ramírez, 1997). It behaves as a seasonal wetland whose flooding is mainly controlled by fluvial and rainfall inputs, desiccation occurs mainly through evapotranspiration during the summer as typically happens in Mediterranean contexts (Rodríguez Ramírez, 1997). The low-altitude areas in the mouth of the Guadalquivir surroundings (0–1.5 m asl) have a long flooding period and are subject to marine influence. The higher altitude areas in the W and NW part of the marshlands (1.5–3 m asl) (Fig. 1c) are deprived from marine influence and flood through aquifer discharge, rainfall and fluvial input, presenting a shorter flooding period (Rodríguez Ramírez, 1997).

The hydrological network within the marshland is articulated around microtopographical elements. The so-called “lucios” (depressions) (Fig. 1c) behave as isolated seasonal lagoons and they are the last areas to desiccate in summer. They host very rich macrophyte communities of *Myriophyllum*, *Potamogeton*, *Ranunculus* subgen. *Batrachium*, *Callitriche* and *Isoetes* (Fig. 1c). The “caños” and “quebradas” are large water channels within the marshes whose margins are covered by Cyperaceae (*Scirpus maritimus*, *S lacustris* and *S littoralis*). The “paciles” and “vetas” are the highest

97 elevation enclaves (1–3 m asl) (Fig. 1), and they host Chenopodiaceae-dominated halo-nitrophilous
98 formations (López Albacete, 2009, Rivas Martínez et al., 1980).

99 An aeolian complex system of littoral origin and a spit barrier separating the marshlands from
100 the sea include the terrestrial communities confining the western Guadalquivir marshes (Fig. 1c and
101 d). The aeolian field includes both stabilised and mobile dune systems. The stabilised systems
102 comprise ancient dunes spanning inland in the E-NE limit of the marshlands. Their vegetation, known
103 as "cotos", is of extensive parkland formations. *Juniperus phoenicea* ssp. *turbinata* and monte blanco
104 (Lamiaceae and Cistaceae scrub) dominate in xerophytic enclaves, while cork oak (*Quercus suber*),
105 *Pinus pinea* and monte negro (Ericaceae and Oleaceae scrub) thrive in moister areas (Fig. 1c and d).
106 Gorses (*Ulex*, *Stauracanthus*, *Genista*) are also prominent elements of the "cotos" understorey.
107 Seasonal ponds and lagoons emerge in the dune depressions during the wet season (López Albacete,
108 2009, Rivas Martínez et al., 1980).

109 The mobile dune system is structured in parallel dune trains that advance westwards into the
110 marshlands running over the palaeoestuary spit barrier. The dune crests are dominated by
111 psammophilous communities of *Ammophila arenaria*, *Artemisia crithmifolia*, *Armeria pungens* and
112 *Juniperus phoenicea* ssp. *turbinata*. The interdunal valleys are covered by *Pinus pinea* (Fig. 1c) that
113 becomes buried in the leeward side of the advancing dunes regenerating towards the windward side
114 of the precedent dune (López Albacete, 2009) (Fig. 1d). Current recruitment of *Pinus pinea* in the area
115 is mostly related to groundwater level, occupying intermediary sandy ridges at the dune slacks. This
116 position allows saplings to escape flood and drought (Muñor-Reinoso and de Castro, 2005) (Fig. 1).

117 The DNP is under Mediterranean climate, with mild winters and hot and dry summers. Mean
118 annual temperature is 16.7 °C, with average maximum temperatures of 24.1 °C in the hottest month
119 (July) and average minimum temperatures of the coldest month (December) of −0.3 °C (Palacio de
120 Doñana weather station; Yll et al., 2003). Precipitation, averaging 542.8 mm/yr (period 1978–2007;
121 Palacio de Doñana weather station) falls mostly in autumn and winter. SW winds are prevalent in the
122 area with an incidence of 22.5% of the days in this direction (Jiménez-Moreno et al., 2015).

123 *2.2. Coring, sedimentological analysis and radiocarbon dating*

124 The Lucio de la Cancela de la Aulaga (LuCA, 36° 59′ 50.99″ N, 6° 25′ 48.67″ W, Datum WGS84, 0 m asl)
125 is a small depression in the western margin of the marshlands (Fig. 1c). A 709 cm-long sediment core
126 was retrieved from the central part of the depression using a mechanical percussion corer in
127 September 2012. The sediment core sections were placed in plastic boxes, protected in plastic
128 guttering and stored under cold conditions prior to laboratory sediment visual description and sub-
129 sampling. Shell remains (shells and shell fragments) presence was recorded in the sub-samples. The

topmost part of the core (< 42 cm) was discarded due to sediment mixing (Fig. 2). Six samples were AMS radiocarbon dated at two laboratories (Poznan Radiocarbon Laboratory in Poland, and ETH Laboratory of Ion Beam Physics in Switzerland) (Table 1). The analyses were performed on total organic carbon and dates were calibrated using both the IntCal13.14C and the Marine13 calibration curves (Reimer et al., 2013). Age-depth modelling was performed by means of linear interpolation using the CLAM package for R (Blaaw, 2010) (Fig. 3).

Grain-size distribution analysis was measured on 88 samples at the MNCN-CSIC (Madrid, Spain) using a Coulter LS 130 laser particle size analyser over the particle size range of 0.38–2000 µm. GRADISTAT software was used for the analysis of the resulting raw data (Blott and Pye, 2001). Values were transformed into the equivalent phi value ($\Phi = -\log_2 D$, D = grain diameter in mm). Skewness, kurtosis and sorting (standard deviation) calculations follow the methodology of Folk and Ward (1957). Suite statistic bi-scatter plots (Tanner, 1991) have been used to correlate the summary statistics with the depositional evolution of the Guadalquivir estuarine environment.

Magnetic susceptibility (mag. sus.), organic matter (org. M) and calcium carbonate ($CaCO_3$) contents were measured on 30 samples at Brunel University London (UK). Mag. sus. was performed using a Bartington MS2 susceptibility meter with the MS2B sensor in dried bulk samples packaged in 10 cm^3 plastic pots at room temperature. The measurements were done at low frequency and with the 0.1 sensitivity setting. All samples were measured twice with air readings before and after for drift correction. The average value of the two corrected measures was taken as the final value (κ). The κ values were normalised to sample mass (χ in $m^3\ kg^{-1}$). Org. M and $CaCO_3$ contents were obtained through loss-on-ignition (LOI) at temperatures of 550 and 950 °C respectively (Heiri et al., 2001).

2.3. Palynological analysis

Palynological analysis was performed at the Universidad de Murcia (Spain) using a sediment volume of ~3 cm^3 in 88 samples. The chemical treatment involved HCl for the dissolution of carbonates, NaOH for the removal of organic matter, and HF for the elimination of silicates (Moore et al., 1991). Heavy liquid ($ZnCl_2$) density separation (Erdtman, 1979) was also done. Tablets with known concentration of *Lycopodium* spores were added at the beginning of the treatment for concentration estimates (Stockmarr, 1971). Identification and counting were completed at ×400 magnification on a light microscope, and at ×1000 using immersion oil when required, supported by the Universidad de Murcia reference collection, keys, and atlases (Díez et al., 1987, Faegri and Iversen, 1989, Moore et al., 1991, Reille, 1995, 1992, Saenz Laín, 1982). Plant nomenclature follows Flora Ibérica (www.floraiberica.es). Non-pollen palynomorphs (NPP) nomenclature largely follows van Geel (2001). Terrestrial pollen sum (TPS) consisted of at least 200 pollen grains of upland taxa (average = 232; median = 222), excluding

Chenopodiaceae (local marshland vegetation), aquatic pollen types, and NPP. Percentages of fern and bryophyte spores, as well as fungal and microfaunal NPP were calculated based on the TPS. The variation of aquatic taxa in the Doñana transitional environments may provide ecological indication. For such reason, percentages of aquatic taxa such as algae, macrophytes, helophytes and Chenopodiaceae were calculated independently based on the aquatic taxa sum (ATS; average = 439; median = 245). Palynological results were plotted in diagrams using Tilia 1.7.16 (Grimm, 2011).

Microcharcoal particles (<125 µm) were counted on the palynological slides, measuring the longest axis (Mooney and Tinner, 2011). A minimum of 200 items (microcharcoal particles and *Lycopodium* spores) was considered per sample (Finsinger et al., 2004).

2.4. Numerical analyses

Palynological zones were identified separately for the terrestrial and aquatic data-sets by stratigraphically constrained cluster analysis by sum-of squares (CONISS) using Tilia 1.7.16 (Grimm, 2011). The analyses included the square-root transformation of terrestrial pollen percentages larger than 10%, and of aquatic taxa percentages larger than 5%.

Non-metric multidimensional scaling (NMDS) analyses were performed on the terrestrial and aquatic data-sets independently to identify those pollen samples with similar taxonomical assemblages and to unravel terrestrial and aquatic vegetation dynamics. Only taxa with percentages larger than 5% were considered (15 terrestrial taxa and 12 aquatic taxa). Bray-Curtis dissimilarity was used to calculate the distance matrix for ordination. NMDS was performed in R using the vegan package (Oksanen et al., 2012).

3. Results

3.1. Sedimentology and age-depth model

The LuCA sediment core presents three packages of blueish (709–480 cm), grey (480–180 cm) and brown (180–0 cm) silts, separated by soft transitions (Fig. 2). Some soft packages, as well as oxidised levels and air inclusions have been found embedded in the core. Grain size distributions are mostly symmetrical (61 samples), although 14 samples are finely skewed, 13 samples coarsely skewed and 1 sample very finely skewed. Sorting (standard deviation) of grain size distributions is poor to very poor (Fig. 4). Content in sand is higher at the core bottom (709–460 cm, average = 18%) with relative maxima at 702, 692, 685, 675, 668–654, 594, 572, 532 and 54 cm depth (a-i events in Fig. 4). Sand content above 460 cm is lower (average = 6.7%). Clay content is around 12.7% at the bottom of the sequence, whereas it doubles above 460 cm (24.8%), with a maximum of 49.1% at 333 cm (Fig. 4).

Suite analysis identifies most of the samples as derived from a partially open to restricted estuarine environment. However, a few samples from the upper 400 cm are indicative of a closed basin (Fig. 5).

The content in $CaCO_3$ oscillates between 8 and 12% from the bottom of the core up to 355 cm, with a minimum of 1.46% at 658 cm depth. A decreasing trend is recorded in the upper 355 cm (Fig. 4). In contrast, org. M content varies between 6 and 7% at the bottom of the sequence, experiencing a gradual increase towards the top. Mag. sus. Presents values ranging at 8–18 × 10^{-8} m^3 kg^{-1}, with a peak at 246–210 cm (21–24 × 10^{-8} m^3 kg^{-1}) (Fig. 4).

Because the shell remains appear from 355 cm depth to the bottom of the sequence (Fig. 2, Fig. 4), the radiocarbon dates (Table 1) from the topmost 355 cm were calibrated using the IntCal13.14C calibration curve; while those dates at depths >355 cm were calibrated using the Marine13 one (Reimer et al., 2013). After calibration, one date (ETH-57406, Table 1) was disregarded for being too old. A slump was excised at 668–652 cm depth (Fig. 3, see Discussion section for further details). An Age-depth model was built by linear interpolation (Fig. 3) and it indicates that the LuCA sedimentary sequence was deposited from ~9.9 to 6.4 cal. kyr BP.

3.2. Terrestrial assemblages

Terrestrial pollen concentration averages values of 11,847 pollen grains g^{-1} (Fig. 4). Concentrations are higher at the 350–193 cm depth interval with average values of 23,093 pollen grains g^{-1}. Three barren samples detect a palynological hiatus at 118–102 cm depth (Fig. 4, Fig. 6). The terrestrial pollen assemblages show a relative stability lacking marked shifts. Evergreen *Quercus* and *Pinus pinea/halepensis* type dominate the arboreal pollen (AP), while Poaceae and Cichorioideae are the main components of the non-arboreal pollen (NAP). Four terrestrial pollen zones have been identified (zones LuCA-T1 to LuCA-T4) (Fig. 6).

In zone LuCA-T1 (710–640 cm depth; 9930–8787 cal. yr BP), evergreen *Quercus* (10–25%) and *Pinus pinea/halepensis* type (10–20%) are the main AP taxa (Fig. 6a), with the significant presence of *Quercus suber* (2–10%). Mesophilous taxa, such as deciduous *Quercus*, also appear. The occurrence of *Pinus pinaster* and *Cedrus* is sparse but continuous. Scrubs are dominated by *Erica* type (5%), with the presence of *Juniperus*, *Olea*, *Phillyrea*, *Pistacia*, *Cytisus/Genista* type and Cistaceae (*Halimium/Helianthemum* type, *Cistus* type and *Cistus ladanifer* type) (Fig. 6a). Poaceae is the main herbaceous taxa, with Cichorioideae, *Aster* type and *Artemisia* presenting moderate percentages (Fig. 6b). Highest percentages (over a 100% of the TPS) of indeterminate fungal spores are registered during zone LuCA-T1 (Fig. 6c).

The zone LuCA-T2 (640–445 cm depth; 8787–7908 cal. yr BP) presents similar evergreen (*Pinus pinea/halepensis* type, evergreen *Quercus* and *Quercus suber*) and mesophilous (deciduous *Quercus*

mainly) AP assemblages than LuCA-T1. Other mesophilous taxa are also present. *Fraxinus* shows continuous curves, while *Alnus*, *Betula* and *Corylus* presences are scattered. The main differences with zone LuCA-T1 are the lower values of Poaceae and the higher ones of Cichorioideae and shrubs, with *Erica* type, *Juniperus*, Cistaceae and *Phillyrea* showing the largest proportions (Fig. 6a and b). *Cedrus* percentages are highest in this zone while indeterminate fungal spores show a decreasing trend (Fig. 6c).

The most characteristic feature of zone LuCA-T3 (445–118 cm depth; 7908–7117 cal. yr BP) is the increase in herbaceous and shrub taxa. Cichorioideae presents its highest percentages, Poaceae remaining with the same values (Fig. 6b). *Juniperus*, *Tamarix*, *Cytisus/Genista* type, *Erica* type and Cistaceae values increase, *Quercus suber* shows lower percentages. *Betula*, *Corylus* and *Taxus* show discrete occurrences, while *Alnus*, *Pinus nigra/sylvestris* type and *Fraxinus* curves are continuous. Poaceae values peak at the zone top (Fig. 6b). Maximum values of microcharcoal concentrations are registered during this zone (Fig. 6c).

The zone LuCA-T4, (102–42 cm depth; 6985–6484 cal. yr BP) is characterised by high values of Poaceae (Fig. 6b). Increasing values of *Pinus pinea/halepensis* type are recorded, in contrast with lower percentages of evergreen *Quercus* type and *Quercus suber*. Overall, tree percentages are at the lowest and shrubs present increasing values, mostly *Juniperus* and *Erica* type. Most mesophytes and *Pinus pinaster* are absent from this zone (Fig. 6a). Maximum values of *Pseudoschizaea circula* and discrete peaks of *Glomus* occur during this zone (Fig. 6c).

3.3. Palaeolimnological assemblages

The concentration of aquatic palynomorphs averages values of 33,795 palynomorphs g^{-1} (Fig. 4). Concentrations increase at the 287–193 cm depth interval (average = 100,639 palynomorphs g^{-1}). The aquatic assemblages, contrary to the terrestrial ones, do not show an apparent stability. Notable fluctuations have been detected, highlighting the presence of two alternating palaeolimnological assemblages. Three aquatic zones have been identified (zones LuCA-A1 to LuCA-A3) (Fig. 6).

The zone LuCA-A1 (710–652 cm depth; 9930–9041 cal. yr BP) shows high values of macrophytes, mainly *Isoetes* Other macrophytes are *Myriophyllum alterniflorum* type, Potamogetonaceae, Ranunculaceae, *Hydrocharis morsus-ranae*, *Callitriche*, *Nymphaea*, *Ricciocarpos*, *Riella* and Zannichelliaceae (Fig. 6). Helophytes such as Chenopodiaceae and Cyperaceae present relatively high percentages; as well as the algae Chlorophyta, Zygnemataceae and *Botryococcus* (Fig. 6).

In zone LuCA-A2 (652–292 cm depth; 9041–7863 cal. yr BP) helophyte and algae values are similar to zone LuCA-1. *Isoetes* has declining values coeval to a rise in Ranunculaceae percentages.

Callitriche, *Hydrocharis morsus-ranae*, *Lemna*, *Riella*, *Ricciocarpos*, and Zannichelliaceae present scattered occurrences (Fig. 6d).

The zone LuCA-A3 (292–42 cm depth; 7863–6487 cal. yr BP) shows the alternation of *Myriophyllum alterniflorum* type/Ranunculaceae-dominated phases (I, III, V and VII) and *Isoetes*/Chenopodiaceae-dominated ones (II and IV). Phase VI (Fig. 6), contains the palynological hiatus (118–102 cm depth).

3.4. Spatiotemporal change in the vegetation structure

NMDS ordination was performed to assess the degree of similarity between contiguous samples and evaluate the spatiotemporal vegetation stability (Fig. 7). Upland vegetation shows long-term stability during more than three millennia (Fig. 7, Fig. 8), and the small-scale fluctuations are most likely related to changes in the phreatic level. The upland taxa with NMDS1 positive loadings (Cichorioideae, *Aster* type, *Cistus* type, and evergreen *Quercus*, Fig. 7) thrive in phreatic water-restricted enclaves, many as part of the monte blanco scrub (Rivas Martínez et al., 1980, López Albacete, 2009) (Fig. 1c and d). Taxa presenting NMDS1 negative loadings (Fig. 7) are associated with higher phreatic layer, vernal pools and groundwater discharge areas, such as *Quercus suber*, deciduous *Quercus* and *Tamarix*, together with the monte negro scrub (*Erica* type, *Cytisus/Genista* type, *Olea*, *Pistacia*) (Fig. 1c and d). Although *Juniperus* populates xerophytic enclaves (Fig. 1) in the Doñana area, it is also related with the local availability of high phreatic layer enclaves (Muñoz Reinoso, 2001, Muñoz-Reinoso and García Novo, 2005). Lastly, *Pinus nigra/sylvestris* type is considered extra-local (long-distance pollen dispersal) Nonetheless, in agreement with the negatively loaded taxa its extant distribution is also restricted by groundwater availability (Blanco et al., 2005).

Aquatic vegetation shows two well-differentiated assemblages (Fig. 7). Vivacious taxa (non-woody taxa that present a pluriannual life cycle) or taxa forming underground resistance structures show positive NMDS1 loadings (Fig. 7): Chenopodiaceae species thrive in salt accumulating soils (García Viñas et al., 2005, Muñoz-Rodríguez et al., 2017, Rivas Martínez et al., 1980), Cyperaceae colonise shallow and marginal environments within the marshland, and *Isoetes* live in waterlogged vernal areas (García Murillo et al., 2014, Molina et al., 2011, Rivas Martínez et al., 1980). Their distribution within the Doñana aquatic environments points to a retraction of flooded areas. Association with Potamogetonaceae, *Lemna* and *Botryococcus*, indicates the survival of shallow slow-running, eutrophic waters, and permanent ponds (García Murillo et al., 2006, 2014, van Geel, 2001, van Wijk, 1988, van Wijk et al., 1988). The macrophytes *Myriophyllum alterniflorum* type and Ranunculaceae, the benthic algae *Gloeotrichia* and Zygnemataceae as well as Chrysophyceae, present negative NMDS1 loadings. In Doñana, *Myriophyllum alterniflorum* and *Ranunculus* subgen.

Batrachium dominate seasonally flooded areas. During the inundation period, macrophyte blooms deplete the water-dissolved nutrients (Bernués, 1990), so filamentous algal developments are restricted to the benthos (Scott and Marcarelli, 2012, Sánchez Castillo, 2015). Under this weakly buffered environment, Chrysophyceae development, indicative of pH changes (Siver, 1995), is promoted. During summer desiccation, macrophytes survive mainly in the form of seeds (van Wijk, 1988) whereas filamentous algae produce cysts. Overall, this assemblage represents seasonally fluctuant, stagnant and deep, environments.

4. Discussion

4.1. Problems of chronological models in transitional environments

Obtaining accurate chronological frameworks in marine-terrestrial transitional contexts is challenging due to the hard-water and the marine reservoir combined effects. The difficulty of determining whether sediments are of terrestrial, marine or transitional origin hinders the selection of the appropriate calibration curve when calibrating radiocarbon measurements. Wetland vegetation is a source of hard-water effect whose magnitude has not been measured for the LuCA sediment record due to the lack of datable terrestrial macro-remains. To minimise this problem, the levels chosen for radiocarbon dating are those in which aquatic palynomorphs were lower. The magnitude and application of the marine reservoir effect (R) in the Gulf of Cadiz have been source of investigation in the last years (Lario et al., 2010a, 2010b, Rodríguez-Ramírez, 2010, Rodríguez-Ramírez et al., 2009, Rodríguez-Ramírez and Yáñez-Camacho, 2008, Rodríguez-Vidal et al., 2009). The marine reservoir value changes through time (Soares and Dias, 2006, Lario et al., 2010a, Lario et al., 2010b) and the cited literature is restricted to the last six millennia. The LuCA sequence covers earlier chronologies, preventing the inclusion of regional ΔR values in the age-depth model. However, a marine influence on the estuary is detected below 355 cm depth with the presence of shell remains.

In addition to the problem of the reservoir effect in marine-terrestrial transitional contexts, sediment accumulation rates can be interrupted in these very dynamic environments by punctual high-energy events (e.g. storms and tsunamis) that may produce abrupt deposition events (slumps). In the case of the LuCA record, particle size distribution (Fig. 4) and suite analysis (Fig. 5) have identified nine abrupt inputs of coarser materials (Fig. 4, Fig. 8), although only one of them (668–652 cm depth interval) is significant enough to be incorporated as a slump in the age-depth model (Fig. 3, Fig. 4, event e).

We agree with Lario et al. (2010a) that future improvements in the methods, calibration curves and modelling techniques will mean the refinement of previous age-depth models for this area.

In the meantime, we favour a more simplistic chronology, knowing the limitations. The chronology of the input of coarser material detected by particle size analysis (Fig. 4, Fig. 5) in the LuCA core shows strong correlation with the turbidite events detected by Gràcia et al. (2010). The chronological models in Gràcia et al. (2010) are built upon marine foraminifera, using the marine calibration curve and corrected for regional ΔR minor disagreements between the chronology of the LuCA and the turbidite events (Fig. 8) might be related to the reservoir effect, the inherent uncertainties of the radiocarbon ages, and/or the fact that these independent chronological models derive from different sedimentological contexts.

4.2. High-energy events in the Guadalquivir palaeoestuary

Storm and tsunamigenic deposits possess similar sedimentary features (Gràcia et al., 2010, Jaffe et al., 2008, Lario et al., 2010b, 2011, Morton et al., 2007, 2008). On-shore deposits only store the occurrence of extreme marine energy wave events (Lario et al., 2011). The correlation of on-shore deposits with the off-shore turbidite record is needed to assess the tsunamigenic origin of sedimentary changes (Gràcia et al., 2010, Lario et al., 2011). The LuCA sediment core records nine sandier events likely related to high energy inputs (Figs. 4 events a–i, Fig. 5, Fig. 8). Four coarser intrusions have been detected at ~9.9–9.2 cal. kyr BP (Figs. 4, events a–d, and 8). The lack of correlation between event b and the turbidite record (Gràcia et al., 2010) as well as the presence of shell fragments point to a storm origin of event b (~9.6 cal. kyr BP), whereas the origin of a, c and d is unclear regarding the available evidence.

A 16-cm thick package containing over 40% sand is recorded at ~9.1 cal. kyr BP (Figs 4, event e, and 8). Suite analysis reveals the highest depositional energy for the LuCA sequence (Fig. 5). The high sand content, together with the presence of shell fragments, most likely indicates an abrupt deposition of marine materials. This event falls within the temporal window of the E10 turbidite (~9.7–9.1 cal. kyr BP; Gràcia et al., 2010) (Fig. 8), thus supporting the tsunamigenic origin of this 16-cm thick package.

A generalised erosive process of the Guadalquivir watershed is manifested by high sedimentation rates at ~8.2–7.8 cal. kyr BP. Three inputs of coarser material are detected at ~8.2–8.0 cal. kyr BP (Figs. 3, events f–h, and 8). Uncertainty about the origin of turbidite event E9, around the 8.2 cal. kyr BP event (Gràcia et al., 2010) (Fig. 8) prevents further conclusions of the origin of these events.

Turbidite event E8 (~6.9–6.6 cal. kyr BP; Gràcia et al., 2010) has been associated with a palaeotsunami occurring at ~7.0–6.8 cal. kyr BP (Lario et al., 2011). LuCA event i chronology (Fig. 4, Fig. 8) broadly agrees with E8, however, it does not feature mollusc bioclasts and presents a moderate

sand content in comparison with the previous extreme wave events. Probably this is due to the enclosure, and consequent protection of the basin (Fig. 5, Fig. 8). However, abrupt changes in the aquatic vegetation provide further evidence of a perturbating event, probably a palaeo-tsunami (Fig. 8).

4.3. Early to mid-Holocene Doñana landscape history

4.3.1. Early Holocene tsunamigenic impacts on the landscape

The Late Pleistocene-Early Holocene development of the Doñana spit barrier and the resulting protection of the lagoon at the mouth of the Guadalquivir frames the development of the early LuCA basin (Ruiz et al., 2010). Its present position within the marshlands of the Guadalquivir complex alludes to an intermediate position between two NW-SE confluent tidal channels during the Early Holocene (Rodríguez-Ramírez et al., 1997, Ruiz et al., 2010). Under these palaeogeographic circumstances, *Isoetes* dominance (Fig. 6, Fig. 8) indicates the prevalence of shallow waterlogged environments in the small basin (Cirujano et al., 2014, Smolders et al., 2002). The relatively high diversity of macrophytes (Fig. 6) points to a large heterogeneity within the LuCA limnic network (Cirujano et al., 2014, García Murillo et al., 2006). At this point, millennial persistence of *Isoetes*-dominated assemblages can be attributed to this spatial heterogeneity and mechanisms of stress survival (i.e. resistance forms - anatomical attributes such as spores, corms, turions, etc. that are related to survival during ecologically unfavourable periods - and propagule bank development) (Cirujano et al., 2014, van Wijk, 1988). Quick colonisation processes explain why neither the gradual embankment nor punctual events such as the 9.1 cal. kyr BP tsunami (Fig. 8) or other extreme wave events seem to produce long-lasting or major changes in the structure of the Early Holocene LuCA aquatic assemblages (Fig. 6, Fig. 8).

Contrastingly, Early Holocene stability of the *Pinus-Quercus* assemblages is disrupted by the 9.1 cal. kyr BP tsunami with a rise in Poaceae (Fig. 8). Sea-water inundation is shown to have varying impacts on different components of the terrestrial subsystem (Miyamoto et al., 2004, Wu and Dodge, 2005). Ecological traits such as salt tolerance, life-span and population turnover amongst terrestrial taxa account for differences in individual responses. For instance, regression is more pronounced in salt-sensitive taxa (evergreen *Quercus*, likely *Q. ilex* and *Q. coccifera*) and seeders (monte blanco vegetation components) (Fig. 8), due to seed bank burial/destruction (Miyamoto et al., 2004, Wu and Dodge, 2005). Conversely, more salt-tolerant taxa (*Pinus pinea* and *Quercus suber*) and sprouters (monte negro vegetation components) are less affected by sea water inundation (Fig. 8) (Miyamoto et al., 2004, Wu and Dodge, 2005).

Overall, following our chronological model, terrestrial woody cover seems to take around 200 years to recover to the 9.1 cal. kyr BP tsunami (Fig. 8), probably due to longer life cycles and slower

colonisation rhythms from more distant inland sources. Aquatic communities, under partially opened and connected basin conditions, are shown to recover much faster due to downstream recolonisation (Fig. 8).

4.3.2. Mid-Holocene ecosystem dynamics: Terrestrial stability versus aquatic vulnerability

The Mid-Holocene onset is marked by a rise in sediment accretion rates, attributed to generalised erosion of the Guadalquivir watershed. Even if the echo of the 8.2 cal. kyr BP global event is not as marked in southern Iberian records as in the northern ones (i.e. González-Sampériz et al., 2006, 2009, López-Merino et al., 2012, Moreno et al., 2011), the location of the estuary at the mouth of the Guadalquivir might amplify the otherwise subtle response of the southern Iberian records to the increase of aridity (and subsequent eolian erosion) associated to this event.

Enhanced sedimentation and concomitant sea-level rise resulted in a reduction of the depositional energy of the LuCA basin from the onset of the Mid-Holocene (blue polygon in Fig. 5) (Dabrio et al., 2000, Rodríguez-Ramírez et al., 1997, Ruiz et al., 2010, Zazo et al., 1994). It is at this time when the LuCA basin becomes a closed environment (red polygon in Fig. 5, Fig. 8). Indeed, lucios (Fig. 1) develop as closed environments behind the confluence of watercourse-flanking levées (Rodríguez-Ramírez et al., 1997). From ~8 cal. kyr BP onwards, intense and frequent marshland vegetation fluctuations point to successive episodes of enclosure and re-opening of the LuCA basin (Fig. 8), although the mechanisms underlying these transitions are difficult to ascertain. Changes in the balance between freshwater supply, sediment accretion rate, subsidence, and sea level rise are the most likely drivers of these changes.

From the second enclosure episode onwards, *Myriophyllum alterniflorum* type/Ranunculaceae-dominated communities, and Chenopodiaceae/Cyperaceae/*Isoetes*-dominated communities, alternate under closed and partially open/restricted conditions respectively (Fig. 8). Major changes in vegetation composition and structure couple with sedimentary basin configuration (Fig. 8). Amplitude of the vegetation response shows the elasticity of aquatic communities to changes in the morpho-sedimentary environment.

Aquatic plants live in micro-environmentally very heterogeneous and fluctuating habitats in the Mediterranean (Díaz-Paniagua et al., 2015, Molina et al., 2011), hence taxa with different ecology may co-exist in the same water bodies (López Albacete, 2009, Lumbreras et al., 2009, 2012, 2013). The resilience of the aquatic communities in the Doñana area depends on the high diversity of long viability diaspores and the resistance structures that accumulate in the sediments (Grillas et al., 1993). The LuCA sequence depicts how small changes in the aquatic environment trigger the trespassing of

environmental thresholds activating drastic, quick changes in the structure and composition of the aquatic vegetation.

Upland vegetation remains practically unaltered through the 8.2 cal. kyr BP event and thereafter during the Mid-Holocene, despite small fluctuations are also recorded (Fig. 8). Vegetation assemblages dominated by *Pinus*, *Quercus*, and *Juniperus* are time transgressive (Fig. 8, Fig. 9) Local geomorphological dynamics have proven to drive small-scale building and destruction of tree prone habitats (López Albacete, 2009, Muñoz Reinoso, 2001, Muñor-Reinoso and de Castro, 2005, Muñoz-Reinoso and García Novo, 2005). This steady ecosystem rejuvenation translates in relatively stable pollen spectra for the dominant trees: *Pinus pinea* and evergreen *Quercus* (Fig. 8) However, the dynamics of *Quercus suber* and *Juniperus* suggest major episodes of geomorphological rejuvenation and variation during the Mid-Holocene that mirror in changes of the aquatic communities (Fig. 8).

4.3.3. Mid-Holocene terrestrial-estuarine connectivity

Two *Juniperus* species coexist in the study area. *J. oxycedrus* ssp. *macrocarpa* lives under sea-sprayed stations, while *J. phoenicea* ssp. *turbinata* creeps on dunes in on-shore, xerophytic enclaves (López Albacete, 2009, Rivas Martínez et al., 1980) (Fig. 1d). The presence of *Juniperus* in LuCA is most likely related to the former species in relation to the inland palaeogeographical position of LuCA. From ~ 7.8 cal. kyr BP, recurrent episodes of *Juniperus*, with a probable ~ 200–400 years periodicity following our chronological model, suggest dune development periods. Dune development is promoted under arid, wind-enhanced conditions (Dabrio et al., 1996, Díaz-Paniagua et al., 2015). However, the dune domes, despite being xerophytic enclaves (Muñoz Reinoso, 2001, Muñor-Reinoso and de Castro, 2005, Muñoz-Reinoso and García Novo, 2005) function as recharge areas and extend the Doñana aquifer volume (Manzano et al., 2013). Expectedly, dune development periods correspond with closed basin episodes (Fig. 8). Aridity translates in a decrease in water supply to the local environments. This would prevent the connection of marginal, marshland areas with the central Guadalquivir mouth. However, groundwater discharges supply the seasonally constrained *Myriophyllum*-Ranunculaceae assemblage.

Coupling between the response of aquatic and terrestrial assemblages from ~7.8 cal. kyr BP onwards (Fig. 8) supports the view that terrestrial-estuarine connectivity is mediated by groundwater discharges, and ultimately controlled by dune configuration. Previous ~200–400-year periodicity in beach ridges evolution has been associated with solar spot cycles (Zazo et al., 1994), which have, in turn, been related to arid events in the Doñana area (Díaz-Paniagua et al., 2015). Solar forcing, through its effect on the dominant winds seems to be the most prevailing controlling factor on the Mid-Holocene Doñana environment (Díaz-Paniagua et al., 2015).

4.3.4. Post-Flandrian development and vulnerability to sea energetic events

458 The palynological hiatus located between 102 and 118 cm depth (Fig. 4) may be connected with the
459 Flandrian sea level maximum, occurring locally at ~6.9–6.5 cal. kyr BP (Zazo et al., 2008, 1994, Dabrio
460 et al., 2000). Regionally, the Flandrian highstand marks a tipping point in the sea level rise rate towards
461 a deceleration phase causing a transition from vertical aggradation towards lateral progradation
462 (Dabrio et al., 2000, Zazo et al., 2008). This would have promoted the development of wide estuaries
463 in the mouth of the main rivers of SW Iberia (Rodríguez-Vidal et al., 2014). Retraction of the sea
464 allowed for local recovery of the aquatic assemblages, as the river mouth and the estuary
465 development migrated SW (Rodríguez-Ramírez and Yáñez-Camacho, 2008, Ruiz et al., 2010). After a
466 short Chenopodiaceae/Cyperaceae/*Isoetes* phase, the detachment from the main estuary basin
467 entailed a switch towards groundwater controlled *Myriophyllum*-Ranunculaceae assemblages (Fig. 8).

468 The ~6.5 cal. kyr BP extreme wave event, under closed basin conditions, had a large impact
469 on the LuCA vegetation (Fig. 8). Contrarily to the previous high energy episodes, rapid recovery of the
470 vegetation structure seems to be restrained by the isolation of the LuCA from other areas of the
471 Guadalquivir's complex of ponds, lagoons, marshes and main estuary basin as the mouth of the river
472 and the development of the estuary moved SW.

473 *4.4. Biogeographical remarks of some tree taxa*

474 The ecological role and natural character of *Pinus pinea* in SW Iberia have been debated both in
475 conservation agendas and policy-making (Blanco et al., 2005, López Albacete, 2009, Pérez Latorre et
476 al., 1999, Rivas Martínez, 1987, 2011). The regional palaeobotanical *Pinus* signal suggests the existence
477 of pinelands in Doñana from the Upper Pleistocene to the Holocene (Jiménez-Moreno et al., 2015,
478 López Sáez et al., 2002, Menéndez Amor and Florschültz, 1973, Stevenson, 1984, 1985, Stevenson and
479 Harrison, 1992, Stevenson and Moore, 1988, Yll et al., 2003). The palynological discrimination of this
480 pine species is suggested by the autoecology of *P. pinea* (Blanco et al., 2005, López Albacete, 2009),
481 and supported by the occurrence of *P. pinea* macrofossils (pine cones, bracts, and seeds) in adjacent
482 sites of the Upper Pleistocene (49.2 kyr BP at Gorham Cave, Gibraltar; 18.4 kyr BP at Nerja Cave,
483 Málaga, S Spain), and the Holocene (7.4 and 5.4 cal. kyr BP at Murciélagos Cave, Albuñol, 2.7 cal. kyr
484 BP at Puerto de Santa María, Cádiz, S Spain; Carrión et al., 2008).

485 The presence of other pine species such as *P. pinaster* and *P. nigra* is supported by the
486 presence of pollen of *P. pinaster* and *P. nigra/sylvestris* type (Fig. 9) and their macroremains in coastal
487 areas (García-Amorena et al., 2007, Postigo-Mijarra et al., 2010a, 2010b). Plausibly, *P. pinaster* groves,
488 like the Barreiro fossil grove (7.93–7.43 cal. kyr BP, Tagus estuary, Central Portugal, García-Amorena
489 et al., 2007) (Fig. 1a), or isolated stands, survived the deglaciation along the SW Iberian coast (Carrión
490 et al., 2000). Coastal, low-lying environments were widely spread during the LGM low-stand but

disappeared as the sea level rose (García-Amorena et al., 2007). The extinction of the pollen signal of *P. pinaster* prior to the Flandrian maximum (Fig. 9) suggests the last remaining stands occupied such low and thus, early flooded areas. On the other hand, *Pinus nigra* macroremains found locally, date from MIS 4 and 3, pointing to an earlier retraction of this species from coastal refugia (Postigo-Mijarra et al., 2010a). A prolific fossil record evidences that the past distribution of *P. nigra* well transcends the extant area (Alcalde Olivares et al., 2000, 2004, Desprat et al., 2015, García-Amorena et al., 2007). However, altitudinal migrations during the Holocene reduced the extension of Iberian *Pinus nigra* pinelands (Carrión et al., 2010, Carrión, 2015). It is possible, nonetheless, that some *Pinus nigra* stands remained relict amongst the Guadalquivir flatlands like they nowadays do amongst the *Pinus pinea* forests in the N Iberian Meseta (Franco-Múgica et al., 2004, García-Antón et al., 2011).

The presence of *Taxus* (Fig. 9) agrees with the general trend for this species. Still today, individual stands and small groups of *Taxus* survive isolated in the S Iberian ranges. Scattered remains are found across Iberia showing multiple glacial refugia (González-Martínez et al., 2010, Uzquiano et al., 2015, Magri et al., 2017). However, the low percentages found evidence its punctual representation in the landscape (Abel-Schaad, 2011, Blanco et al., 2005).

Cedrus is another tree taxon worth a discussion. Quaternary macrofossils have never been found, but frequent pollen occurrences along the Tertiary, Pleistocene, and sparser throughout the Holocene are concentrated on the Baetic Ranges (Fierro Enrique, 2014, Magri and Parra, 2002, Postigo-Mijarra et al., 2010b) and northern Iberian mountains (Aranbarri et al., 2014). The palynological detection of *Cedrus* in SW Europe has been attributed to periods of low tree cover (cold and arid periods, Magri and Parra, 2002, Magri et al., 2017). Interestingly, the LuCA record of *Cedrus* takes place at ~8.2–7.7 cal. kyr BP (Fig. 9), just when pollen concentrations are the highest. *Cedars* have been suggested to take part of relicts of tree vegetation persisting hidden in the Baetic Ranges along the Holocene (Postigo-Mijarra et al., 2010b). Our data are inconclusive in this respect, but they may be used to give some support to the hypothesis of Postigo-Mijarra et al. (2010b).

The intermittent presence of *Castanea* provides further evidence of the autochthonous character of the sweet chestnut, and the presence of southern Iberian refuges (Fig. 9; Anderson et al., 2011, Carrión et al., 2008, García-Amorena et al., 2007, Morales-Molino et al., 2011, Pons and Reille, 1988), as well as northern ones (Aranbarri et al., 2016). The Quaternary history of other mesophytes such as *Corylus*, *Betula*, *Ulmus*, *Fraxinus*, *Populus* and *Alnus* is better understood for S Iberia (González-Sampériz et al., 2010, Manzano et al., 2017). Locally, Late Quaternary evidences for these species are also found in El Asperillo (Morales-Molino et al., 2011, Stevenson, 1984) and Mari López (Yll et al., 2003, Zazo et al., 1999). Most of these mesophytes find their SW distribution limits within the Iberian Mediterranean region, generally associated to watercourses (Blanco et al., 2005). Geomorphological

research in Doñana has shown the existence of braided palaeo-channels and depressions during the Late Pleistocene (Zazo et al., 2008). Edaphic compensation in these environments could have supported the presence of relict and refuged trees in Doñana. Their depletion during the Mid-Holocene may be linked to the transition towards a groundwater, and thus rainfall-controlled environment. Episodic dry spells along the Mid- and Late Holocene would have eliminated all but the riparian species that have reached the present (e.g. *Fraxinus*, *Populus*, *Salix*; Carrión et al., 2003, Carrión et al., 2007, López Albacete, 2009).

5. Conclusions

The LuCA palaeoecological sequence is connected with the terrestrialisation of the Guadalquivir palaeoestuary. The Holocene history of Doñana is unavoidably linked to the development of the Doñana spit and the consequent infilling of the estuary. The Early Holocene millennial-scale resilience of the upland and aquatic vegetation for a coastal transitional and therefore geomorphologically dynamic system is therefore striking.

The growth of the spit enclosing the estuary, and the concomitant accumulation of sand, sharply contrasts with the relative stability of upland vegetation. However, substrate dynamism rejuvenates the terrestrial ecosystems through periodic destruction, but also has created novel habitats. At a landscape scale, this ensures millennial-scale resilience of the upland forest vegetation. Connectivity of the LuCA within the heterogenous limnic network ensuring both in situ survival and quick recolonisation processes, is a primary consideration for the Early Holocene marshland vegetation stability.

Contrastingly, from 7.8 cal. kyr BP onwards, after ~400 years of enhanced sedimentation, successive shifts from open to closed sedimentary basin states are associated with abrupt changes in the aquatic communities, alternating between two different vegetation assemblages. These two states are segregated by resistance strategy traits, salt tolerance, water depth, trophic status and hydro-period requirements. Coupling between the ecological trajectories of both the upland and aquatic systems points to a strong terrestrial-estuarine connectivity, channelled through groundwater discharges.

The impact of several high energy events punctuates the Early and Middle Holocene LuCA sedimentary sequence, two of which are synchronous to the local tsunami record (~6.6 and ~9.1 cal. kyr BP). Contrasting impacts of these two events in the aquatic and upland ecosystems manifest the importance of landscape configuration and the contingent history as key elements for coastal protection.

This study contributes to the *Pinus pinea* autochthony debate, and sets the baseline for the understanding of general drivers and forcings directing long-term vegetation change in Doñana. Seemingly, the natural perturbation regime in this area is strongly dependent on wind, uplifting, and moving dunes. In turn, rising dunes expand the aquifer volume and its groundwater recharge, finally nurturing both the terrestrial and aquatic ecosystems. Plausibly, the high biodiversity in Doñana has been favoured by the landscape heterogeneity derived from such geomorphological dynamism and small-scale mosaics, both in the upland and the estuarine-marshland ecosystems.

In conclusion, a geo-biosphere approach is needed to understand the patterns and processes of vegetation change in dynamic transitional systems. Substrate dynamism and habitat destruction are rather friends than foes of Doñana. Future perspectives for biodiversity conservation, coastal protection and ecosystem servicing (groundwater availability) in the DNP may depend upon incorporating these deep time answers for present-time questions.

Acknowledgements

This work has been funded by the national projects CGL-BOS-2012-34717 and CGL 2015-68604 (Ministry of Economy and Competitiveness), 261-2011 (Spanish National Park Autonomous Organism, Ministry of Natural, Rural and Marine Environment) and a grant from Fundación Séneca (ref. 19434/PI/14). SM is supported by a predoctoral contract (BES-2013-062721, Ministry of Economy and Competitiveness). We want to thank S.A.G. Leroy and the Institute of Environment, Health and Societies (Brunel University London) for hosting SM during the org. M, $CaCO_3$, and mag. sus. analysis and J. Lario (Museo Nacional de Ciencias Naturales-CSIC, Madrid) for providing access to the sedimentology facilities of the MNCN-CSIC. We also thank A. Megías-Bas, L. Scott and A.C. van Aardt for hosting SM during the writing of this manuscript, and R.S. Anderson and an anonymous referee for their useful contributions. SM wants to thank the 3OD crew for their support, discussions and interesting insights on biological system interactions and dynamics.

References

Abel-Schaad D. 2011. *Evolución de la vegetación durante el Holoceno reciente en la vertiente extremeña del Sistema Central a partir del análisis palinológico*. PhD Thesis, Universidad de Extremadura

Alcalde Olivares C., García-Amorena I., Gómez-Manzaneque F., Maldonado-Ruiz J., Morla C., Postigo-Mijarra J.M. 2000. A study of fossil plant remains at the archaeological site in Lomilla, Aguilar de Campoo, Palencia, Spain. *An. Jard. Bot. Madr.*, 59 (1), 101-112

590 Alcalde Olivares C., García-Amorena I., Gómez-Manzaneque F., Maldonado-Ruiz J., Morla C., Postigo-Mijarra
591 J.M., Rubiales J.M., Sánchez Hernando L.J. 2004. Nuevos datos de carbones y maderas fósiles de *Pinus*
592 *pinaster* Aiton en el Holoceno de la Península Ibérica. *Investigaciones Agrarias: Sistemas de Recursos*
593 *Forestales, Fuera de serie*, 152-163
594 Anderson R.S., Jiménez-Moreno G., Carrión J.S., Pérez-Martínez C. 2011. Postglacial history of alpine vegetation,
595 fire and climate from Laguna de Río Seco, sierra Nevada, southern Spain. *Quat. Sci. Rev.*, 30, 1615-1629
596 Aranbarri J., González-Sampériz P., Valero-Garcés B., Moreno P., Gil-Romera G., Sevilla-Callejo M., García-Prieto
597 E., Di Rita F., Mata M.P., Morellón M., Magri D., Rodríguez-Lázaro J., Carrión J.S. 2014. Rapid climatic
598 changes and resilient vegetation during the Lateglacial and Holocene in a continental region of south-
599 western Europe. *Glob. Planet. Chang.*, 114, 50-65
600 Aranbarri J., Bartolomé M., Alcolea M., Sancho C., Celant P., González-Sampériz P., Arenas C., Magri D.,
601 Rodriguez-Lázaro J. 2016. Palaeobotanical insights from early-mid Holocene fluvial tufas in the Moncayo
602 Natural Park (Iberian range, NE Spain): regional correlations and biogeographic implications. *Rev.*
603 *Palaeobot. Palynol.*, 234, 31-43
604 Barbier E.B., Hacker S.D., Kennedy C., Koch E.W., Stier A.C., Silliman B. 2011. The value of estuarine and coastal
605 ecosystem services. *Ecol. Monogr.*, 81 (2), 169-193
606 Bernués M. 1990. *Limnología de los ecosistemas acuáticos del Parque Nacional de Doñana*. PhD Thesis,
607 Universidad Autónoma de Madrid
608 Blaaw M. 2010. Methods and code for "classical" age-modelling of radiocarbon sequences. *Quat. Geochronol.*,
609 5, 512-518
610 Blanco E.C., Costa M.T., Morla C.J., Sainz H. 2005. *Los bosques ibéricos. Una interpretación geobotánica* (4th
611 edition), Ed. Planeta, Barcelona
612 Blott S.J., Pye K. 2001. GRADISTAT: a grain size distribution and statistics package for the analysis of
613 unconsolidated sediments. *Earth Surf. Process. Landf.*, 26, 1237-1248
614 Carrión J.S. (Coord.). 2015. *Cinco millones de años de cambio vegetal en la Península Ibérica e Islas Baleares*.
615 Ministerio de Economía y Competitividad, Madrid. Universidad de Murcia y Fundación Séneca, Murcia
616 Carrión J.S., Navarro C., Navarro J., Munuera M. 2000. The interpretation of cluster pine (*Pinus pinaster*) in
617 floristic-phytosociological classifications from a palaeoecological perspective. *The Holocene*, 10, 243-252
618 Carrión J.S., Sánchez-Gómez P., Mota J., Chaín C. 2003. Fire and grazing are contingent on the Holocene
619 vegetation dynamics of sierra de Gádor, southern Spain. *The Holocene*, 13, 839-849
620 Carrión J.S., Fuentes N., González-Sampériz P., Sánchez Quirante L., Finlayson J.C., Fernández S., Andrade A.
621 2007. Holocene environmental change in a montane region of southern Europe with a long history of
622 human settlement. *Quat. Sci. Rev.*, 26, 1455-1475
623 Carrión J.S., Finlayson C., Fernández S., Finlayson G., Allué E., López-Sáez J.A., López-García P., Gil-Romera G.,
624 Bailey G., González-Sampériz P. 2008. A coastal reservoir of biodiversity for late Pleistocene human
625 populations: palaeoecological investigations in Gorham's cave (Gibraltar) in the context of Iberian
626 peninsula. *Quat. Sci. Rev.*, 27, 2118-2135

627 Carrión J.S., Fernández S., González-Sampériz P., Gil-Romera G., Badal E., Carrión-Marco Y., López-Merino L.,
628 López-Sáez J.A., Fierro E., Burjachs F. 2010. Expected trends and surprises in the Lateglacial and Holocene
629 vegetation history of the Iberian peninsula and Balearic Islands. *Rev. Palaeobot. Palynol.*, 162, 458-475
630 Cirujano S., Meco A., García Murillo P., Chirino Argenta M. 2014. *Flora acuática española. Hidrófitos Vasculares*.
631 Gráficas Arias Montano, Madrid (320 pp)
632 Dabrio C.J., Borja F., Zazo C., Boersma J.R., Lario J., Goy J.L., Polo M.D. 1996. Dunas eólicas y facies asociadas
633 pleistocenas y holocenas en el acantilado del Asperillo (Huelva). *Geogaceta*, 20 (5), 1089-1092
634 Dabrio C., Zazo C., Goy J.L., Sierro F.J., Borja F., Lario J., Gonzalez J.A., Flores J.A. 2000. Depositional history of
635 estuarine infill during the last postglacial transgression (Gulf of Cádiz, southern Spain). *Mar. Geol.*, 1162,
636 381-404
637 Desprat S., Díaz Fernández P.M., Coulon T., Ezzat L., Pessarossi-Langlois J., Gil L., Morales-Molino C., M.F.
638 Sánchez-Goñi. 2015. *Pinus nigra* (European black pine) as the dominant species of the last glacial
639 pinewoods in south western to central Iberia: a morphological study of modern and fossil pollen *J.*
640 *Biogeogr.*, 42, 1998-2009
641 Díaz-Paniagua C., Fernandez Zamudio M.R., Serrano Martin L., Florencio Díaz M., Gómez Rodríguez C., Sousa A.,
642 Sánchez Castillo P., García-Murillo P., Siljestrom P. 2015. *El Sistema de Lagunas Temporales de Doñana,*
643 *una red de hábitats acuáticos singulares*. Organismo Autónomo de Parques Nacionales, Ministerio de
644 Agricultura, Alimentación y Medio Ambiente, Madrid
645 Díez M.J., Valdés B., Fernández I. 1987. *Atlas polínico de Andalucía Occidental*. Instituto de Desarrollo Regional
646 y Excma Diputación de Cádiz, Sevilla
647 Erdtman G. 1979. *Handbook of Palynology. An introduction to the study of pollen grains and spores*. Munksgaard,
648 Copenhagen
649 Faegri K., Iversen J. 1989. *Textbook of Pollen Analysis* (Fourth ed). John Wiley & Sons, Chichester
650 Fierro Enrique E. 2014. *Paleoambientes en el sureste de España: Nuevos datos palinológicos y discusión en el*
651 *contexto de la Península Ibérica*. PhD Thesis, Universidad de Murcia
652 Finsinger W., Tinner W., Hu F. 2004. Rapid and Accurate Estimates of Microcharcoal Content in Pollen Slides.
653 *Charcoals from the Past: Cultural and Palaeoenvironmental Implications: Proceedings of the Third*
654 *International Meeting of Anthracology*, Cavallino-Lecce (Italy), pp. 121-124
655 Folk R.L., Ward W.C. 1957. Brazos River bar: a study in the significance of grain size parameters. *J. Sediment.*
656 *Petrol.*, 31, 514-529
657 Franco-Múgica F., García-Antón M., Maldonado Ruiz J., Morla C., Sainz Ollero H. 2004. Ancient pine forest on
658 inland dunes in the Spanish northern meseta. *Quat. Res.*, 63, 1-14
659 García Murillo P., Fernández Zamudio R., Cirujano S., Sousa A. 2006. Aquatic macrophytes in Doñana protected
660 area (SW Spain): an overview. *Limnetica*, 25 (1–2), 71-80
661 García Murillo P., Bazo E., Fernández Zamudio R. 2014. The plants of Doñana National Park's marisma (Spain): a
662 key element for conservation of an emblematic European wetland. *Ciencia UAT*, 9 (1), 60-75

García Viñas J.I., Mintegui Aguirre J.A., Robredo Sánchez J.C. 2005. *La vegetación en la marisma del Parque Nacional de Doñana en relación con su regimen hidráulico.* Naturaleza y Parques Nacionales. Serie Técnica. Organismo Autónomo de Parques Nacionales, Ministerio de Medio Ambiente, Madrid

García-Amorena I., Gómez-Manzaneque F., Rubiales J.M., Granja H.M., Soares de Carvalho G., Morla C. 2007. The late quaternary coastal forests of western Iberia: a study of macrorremains. *Palaeogeogr. Palaeoclimatol. Palaeoecol.*, 254, 448-461

García-Antón M., Franco-Múgica F., Morla C., Maldonado J. 2011. The biogeographical role of *Pinus* forests on the northern Spanish Meseta: a new Holocene sequence. *Quat. Sci. Rev.*, 30, 757-768

van Geel B. 2001. Non-pollen Palynomorphs. In J.P. Smol, H.J.B. Birks, W.M. Last (Eds.), *Tracking Environmental Change Using Lake Sediments. Volume 3: Terrestrial, Algal, and Siliceous Indicators*. Kluwer Academic Publishers, Dordretch, pp. 99-119

González-Martínez S.C., Dubreuil M., Riba M., Vendramin G.G., Sebastiani F., Mayol M. 2010. Spatial genetic structure of I L., ion the western Mediterranean Basin: past and present limits to gene movement over a broad geographic scale. *Mol. Phylogenet. Evol.*, 55, 805-815

González-Sampériz P., Valero-Garcés B.L., Moreno A., Jalut G., García-Ruiz J.M., Martí-Bono C., Delgado-Huertas A., Navas A., Otto T., Dedoubat J.J. 2006. Climate variability in the Spanish Pyrenees during the last 30,000 yr revealed by the el Portalet sequence. *Quat. Res.*, 66, 38-52

González-Sampériz P., Utrilla P., Mazo C., Valero-Garcés B., Sopena M., Morellón M., Sebastián M., Moreno A., Martínez-Bea M. 2009. Patterns of human occupation during the early Holocene in the Central Ebro Basin (NE Spain) in response to the 8.2 ka climatic event. *Quat. Res.*, 71, 121-132

González-Sampériz P., Leroy S., Carrión J.S., García-Antón M., Gil-García M.J., Figueiral I. 2010. Steppes, savannahs and botanic gardens during the Pleistocene. *Rev. Palaeobot. Palynol.*, 162, 427-457

Gràcia E., Vizcaino A., Escutia C., Asioli A., Rodés A., Pallàs R., Garcia-Orellana J., Lebreiro S., Goldfinger C. 2010. Holocene earthquake record offshore Portugal (SW Iberia): testing turbidite paleoseismology in a slow-convergence margin. *Quat. Sci. Rev.*, 29, 1156-1172

Grillas P., García-Murillo P., Geertz-hansen O., Marbá N., Montes C., Duarte C.M., Tan Ham L., Grossman A. 1993. Submerged macrophyte seed bank in a Mediterranean temporary marsh: abundance and relationship with established vegetation. *Oecologia*, 94, 1-6

Grimm E.C. 2011. *Tilia Software V.1.7.16*. Illinois State Museum, Springfield IL

Heiri O., Lotter A.F., Lemcke G. 2001. Loss on ignition as a method for estimating organic and carbonate content in sediments: reproducibility and comparability of results. *J. Paleolimnol*., 25, 101-110

Jaffe B.E., Morton R.A., Kortekaas S., Dawson A.G., Smith D.E., Gelfenbaum G., Foster I.D.L., Long D., Shi S. 2008. Discussion of articles in "sedimentary features of tsunami deposits". *Sediment. Geol.*, 211, 95-97

Jiménez-Moreno G., Rodríguez-Ramírez A., Pérez-Asensio J.N., Carrión J.S., López-Sáez J.A., Villarías-Robles J.J.R., Celestino-Pérez S., Cerrillo-Cuenca E., León A., Contreras C. 2015. Impact of late-Holocene aridification trend, climate variability and geodynamic control on the environment of a coastal area in SW Spain. *The Holocene*, 25 (4), 607-617

Lario J., Dabrio C.J., Zazo C., Goy J.L., Borja F., Cabero A., Bardají T., Silva P.G. 2010a. Comment on "formation of the chenier plain of the Doñana marshland (SW Spain): observations and geomorphic model" by a. Rodríguez-Ramírez, C.M. Yáñez-Camacho [marine geology 254 (2008) 187-196]. *Mar. Geol.*, 275, 283-286

Lario J., Luque L., Zazo C., Goy J.L., Spencer C., Cabero A., Bardaji T., Borja F., Dabrio C.J., Civis J., González-Delgado J.A., Borja C., Alonso-Azcarate J. 2010b. Tsunami vs. storm surge deposits: a review of the sedimentological and geomorphological records of extreme wave events (EWE) during the Holocene in the gulf of Cádiz, Spain. *Z. Geomorphol.*, 54 (Suppl. 3), 301-316

Lario J., Zazo C., Goy J.L., Silva P.G., Bardaji T., Cabero A., Dabrio C.J. 2011. Holocene palaeotsunami catalogue of SW Iberia. *Quat. Int.*, 242, 196-200

López Albacete I. 2009. *La vegetación del manto eólico de Doñana*. PhD thesis, Universidad de Huelva

López Sáez J.A., López García P., Martín Sánchez M. 2002. Palaeoecology and Holocene environmental change from a saline lake in south West Spain: protohistorical and prehistorical vegetation of the Cádiz Bay. *Quat. Int.*, 93-94, 197-206

López-Merino L., Silva Sánchez N., Martínez Cortizas A., Kaal J., López-Sáez J.A. 2012. Post-disturbance vegetation dynamics during the late Pleistocene and the Holocene: an example from NW Iberia. *Glob. Planet. Chang.*, 92-93, 58-70

Lumbreras A., Olives A., Quintana J.R., Pardo C., Molina J.A. 2009. Ecology of aquatic *Ranunculus* communities under the Mediterranean climate. *Aquat. Bot.*, 90, 59-66

Lumbreras A., Tahiri H., Pinto-Cruz C., Pardo C., Molina J.A. 2012. Habitat variation in vernal pool ecosystems on both sides of the strait of Gibraltar. *J. Coast. Res.*, 28 (5), 1032-1039

Lumbreras A., Pardo C., Molina J.A. 2013. Bioindicator role of aquatic *Ranunculus* in Mediterranean freshwater habitats. Aquatic conservation: marine and freshwater. *Ecosystems*, 23, 582-593

Magri D., Parra I. 2002. Late quaternary pollen records from African winds. *Earth Planet. Sci. Lett.*, 200, 401-408

Magri D., Di Rita F., Arambarri J., Fletcher W., Gonzalez-Sampériz P. 2017. Quaternary disappearance of tree taxa from southern Europe: timing and trends. *Quat. Sci. Rev.*, 163, 23-25

Manzano M., Custodio E., Lozano E., Higueras H. 2013. Relationships between Wetlands and the Doñana Coastal Aquifer (SW Spain). In L. Ribeiro, T.Y. Stitger, A. Chambel, M.T. Condesso de Melo, J.P. Monteiro, A. Medeiros (Eds.), *Groundwater and Ecosystems. IAH. Selected Papers on Hydrogeology* 18, 169-182

Manzano S., Carrión J.S., López-Merino L., González-Sampériz P., Munuera M., Fernández S., Martín-Lerma I., Gómez Ferreras M.C. 2017. Mountain strongholds for woody angiosperms during the late Pleistocene in SE Iberia. *Catena*, 149, 701-712

Martí R., del Moral J.C. 2002. *La invernada de aves acuáticas en España. Serie Técnica*. MMA, Madrid

Menéndez Amor J., Florschültz F. 1973. Resultados del análisis paleobotánico de una capa de turba en las cercanías de Huelva (Andalucía). *Estud. Geol.*, 20, 183-186

Miyamoto S., Martínez I., Padilla M., Portillo A., Ornelas D. 2004. *Landscape Plant Lists for Salt Tolerance Assessment*. U.S.D.I. Bureau of Reclamation

Molina J.A., Lumbreras A., Gallardo T., Agostinelli E., Casermeiro M.A., Prada C. 2011. Small-scale Isoetes distribution pattern in a Mediterranean vernal pool system. *Acta Bot. Gallica*, 158, 27-36

738 Mooney S.D., Tinner W. 2011. The analysis of charcoal in peat and organic sediments. *Mires and Peat* 7: Art. 9
739 http://www.mires-andpeat.net/pages/volumes/map07/map0709.php
740 Moore P.D., Webb J.A., Collinson M.E. 1991. *Pollen Analysis, Second ed*. Blackwell Scientific Publications, London
741 Morales-Molino C., Postigo-Mijarra J.M., García-Antón, C. Zazo M. 2011. Vegetation and environmental
742 conditions in the Doñana Natural Park coastal area (SW Iberia) at the beginning of the last glacial cycle.
743 *Quat. Res.*, 75, 205-212
744 Moreno A., López-Merino L., Leira M., Marco-Barba J., González-Sampériz P., Valero-Garcés B.L., López-Sáez J.A.,
745 Santos L., Mata P., Ito E. 2011. Revealing the last 13,500 years of environmental history from the
746 multiproxy record of a mountain lake (Lago enol, northern Iberian peninsula). *J. Paleolimnol.*, 46, 327-
747 349
748 Morton R.A., Gelfenbaum G., Jaffe B.E. 2007. Physical criteria for distinguishing sandy tsunami and storm
749 deposits using modern examples. *Sediment. Geol.*, 200, 184-207
750 Morton R.A., Goff J.R., Nichol S.L. 2008. Hydrodynamic implications of textural trends in sand deposits of the
751 2004 tsunami in Sri Lanka. *Sediment. Geol.*, 207, 56-64
752 Muñor-Reinoso J.C., de Castro F.J. 2005. Application of a statistical water-table model reveals connection
753 between dunes and vegetation at Doñana. *J. Arid Environ.*, 60, 663-679
754 Muñoz Reinoso J.C. 2001. Vegetation changes and groundwater abstraction in SW Doñana, Spain. *J. Hydrol.*, 242,
755 197-209
756 Muñoz-Reinoso J.C., García Novo F. 2005. Multiscale control of vegetation patterns: the case of Doñana (SW
757 Spain). *Landsc. Ecol.*, 20, 51-61
758 Muñoz-Rodríguez A.F., San José I., Márquez-García B., Infante-Izquierdo M.D., Polo-Ávila A., Nieva F.J.J., Castillo
759 J.M. 2017. Germination syndromes in response to salinity of Chenopodiaceae halophytes along the
760 intertidal gradient. *Aquat. Bot.*, 139, 48-56
761 Newton A., Carruthers T.J.B., Icely J. 2012. The coastal syndrome and hotspots on the coast. *Estuar. Coast. Shelf*
762 *Sci.*, 96, 39-47
763 Newton A., Icely J., Cristina S., Brito A., Cardoso A.C., Colijin F., Dalla Riva S., Gertz F., Hansen J., Holmer M.,
764 Ivanova K., Leppäkoski E., Mocenni C., Mudge S., Murray N., Pejrup M., Razinkovas A., Reizopoulou S.,
765 Pérez-Ruzafa A., Schernewski G., Schulbert H., Seeram L., Solidoro C., Viaroli P., Zaldívar J.-M. 2014. An
766 overview of ecological status, vulnerability and future perspectives of European large shallow, semi-
767 enclosed coastal systems, lagoons and transitional waters. *Estuar. Coast. Shelf Sci.*, 140, 1-28
768 Oksanen J., Blanchet G., Kindt R., Legendre P., Minchin P.R., O'Hara R.B., Simpson G.L., Solymos P., Stevens H.H.,
769 Wagner H. 2012. Package "vegan". 2.0-5. Community ecology package for R
770 Pérez Latorre A.V., Galán de Mera A., Cabezudo B. 1999. Propuesta de aproximación sintáxonomica sobre las
771 comunidades de gimnospermas de la provincia Bética (España). *Acta Bot. Malacit.*, 24, 257-262
772 Pons A., Reille M. 1988. The Holocene and late Pleistocene pollen record from (Granada, Spain): a new study.
773 *Palaeogeogr. Palaeoclimatol. Palaeoecol.*, 66, 243-263

774 Postigo-Mijarra J.M., Gómez Manzaneque F., Morla C., Zazo C. 2010a. Palaeoecological significance of late
775 Pleistocene pine macrofossils in the lower Guadalquivir Basin (Doñana natural park, southwestern Spain).
776 *Palaeogeogr. Palaeoclimatol. Palaeoecol.*, 295, 332-343
777 Postigo-Mijarra J.M., Morla C., Barrón E., Morales-Molino C., García S. 2010b. Patterns of extinction and
778 persistence of Arctotertiary flora in Iberia during the quaternary. *Rev. Palaeobot. Palynol.*, 162, 416-426
779 Reille M. 1992. *Pollen et Spores d'Europe et Afrique du Nord*. Laboratoire de Botanique Historique et Palynologie,
780 Marseille
781 Reille M. 1995. *Pollen et Spores d'Europe et Afrique du Nord. Suppl.1*. Laboratoire de Botanique Historique et
782 Palynologie, Marseille
783 Reimer P.J., Bard E., Bayliss A., Beck J.W., Blackwell P.G., Bronk Ramsey C., Buck C.E., Cheng H., Edwards R.L.,
784 Friedrich M., Grootes P.M., Guilderson T.P., Haflidason H., Hajdas I., Hatté C., Heaton T.J., Hoffmann D.L.,
785 Hogg A.G., Hughen K.A., Kaiser K.F., Kromer B., Manning S.W., Niu M., Reimer R.W., Richards D.A., Scott
786 E.M., Southon J.R., Staff R.A., Turney C.S.M., van der Plicht J. 2013. IntCal13 and Marine13 radiocarbon
787 age calibration curves 0–50,000 years cal BP. *Radiocarbon*, 55 (4), 1869-1887
788 Rendón M.A., Green A.J., Aguilera E., Almaraz P. 2008. Status, distribution and long-term changes in the
789 waterbird community wintering in Doñana, south–west Spain. *Biol. Conserv.*, 141 (5), 1378-1388
790 Rivas Martínez S. 1987. *Memoria del mapa de series de vegetación de España*. ICONA. Ministerio de Agricultura,
791 Pesca y Alimentación
792 Rivas Martínez S. 2011. Mapa de series, geoseries y geopermaseries de vegetación de España (Memoria del
793 mapa de vegetación potencial de España). *Itinera Geobotánica*, 18, 1-2 (Tomos)
794 Rivas Martínez S., Costa M., Castroviejo S., Valdés E. 1980. Vegetación de Doñana (Huelva, España). *Lazaroa*, 2,
795 5-190
796 Rodríguez Ramírez A. 1997. *Geomorfología del Paruqe Nacional de Doñana y su Entorno*. Organismo Autonomo
797 de Parques Nacionales. Ministerio de Medio Ambiente, Madrid
798 Rodríguez-Ramírez A. 2010. Comment on “formation of the chenier plain of the Doñana marshland (SW Spain):
799 observations and geomorphic model” by a. Rodríguez-Ramírez, C.M. Yáñez-Camacho [marine geology
800 254 (2008) 187-196]. *Mar. Geol.*, 275, 290-291
801 Rodríguez-Ramírez A., Yáñez-Camacho C. 2008. Formation of the chenier plain of the Doñana marshland (SW
802 Spain): observations and geomorphic model. *Mar. Geol.*, 254, 187-196
803 Rodríguez-Ramírez A., Rodríguez-Vidal J., Cáceres L.M., Clemente L., Cantano M., Belluomini G., Manfra L.,
804 Improta S. 1997. Evolución de la costa atlántica onubense (SO España) desde el máximo flandriense a la
805 actualidad. *Bol. Geol. Min.*, 108 (4–5), 465-475
806 Rodríguez-Ramírez A., Morales J.A., Borrego J., San Miguel E.G. 2008. Reply to the comment on “formation of
807 the chenier plain of the Doñana marshland (SW Spain): observations and geomorphic model” by a.
808 Rodríguez-Ramírez, C.M. Yáñez-Camacho [marine geology 254 (2008) 187-196]. *Mar. Geol.*, 263, 123-125
809 Rodríguez-Vidal J., Ruiz F., Cáceres L.M. 2009. Comment on “formation of the chenier plain of the Doñana
810 marshland (SW Spain): observations and geomorphic model” by a. Rodríguez-Ramírez, C.M. Yáñez-
811 Camacho [marine geology 254 (2008) 187-196]. *Mar. Geol.*, 263, 120-122

812 Rodríguez-Vidal J., Bardají T., Zazo C., Goy J.L., Borja F., Dabrio C.J., Lario J., Cáceres L.M., Ruiz F., Abad M. 2014.
813 Coastal dunes and marshes in Doñana National Park. In F. Gutiérrez, M. Gutiérrez (Eds.), *Landscapes and*
814 *Landforms of Spain. World Geomorphological Landscapes*. Springer, Dordretch
815 Ruiz F., Rodríguez-Ramírez A., Cáceres L.M., Rodríguez-Vidal J., Yañez C., Clemente L., González-Regalado M.L.,
816 Abad M., De Andrés J.R. 2002. Cambios paleoambientales en la desembocadura del río Guadalquivir
817 durante el Holoceno reciente. *Geogaceta*, 31, 167-170
818 Ruiz F., Pozo M., Carretero M.I., Abad M., González-Regalado M.L., Muñoz J.M., Rodríguez-Vidal J., Cáceres L.M.,
819 Pendón J.G., Prudêncio M.I., Dias M.I. 2010. Birth, evolution and death of a lagoon, Late Pleistocene to
820 Holocene palaeoenvironmental reconstruction of the Doñana National Park (SW Spain). In A.G. Friedman
821 (Ed.), *Lagoons: Biology, Management and Environmental Impact*. Nove Science Publishers
822 Saenz Laín C. 1982. Polen de la flora de Doñana (Huelva, España). *Lazaroa*, 2, 191-270
823 Sánchez Castillo P.M., Díaz-Paniagua C. (coord.). 2015. Diversidad Morfológica y estrategias reproductoras en
824 algas filamentosas de las marismas y lagunas de Doñana. In *El Sistema de Lagunas Temporales de Doñana,*
825 *una red de hábitats acuáticos singulares*. Organismo Autónomo de Parques Nacionales. Ministerio de
826 Agricultura, Alimentación y Medio Ambiente, Madrid
827 Scott J.T., Marcarelli A.M., Whitton B. 2012. *Cyanobacteria in freshwater benthic environments. Ecology of*
828 *Cyanobacteria II: Their Diversity in Space and Time*. Springer
829 Siver P.A., Sandgren C.D., Smol J.P., Kristiansen J. 1995. The distribution of chrysophytes along environmental
830 gradients: their use as biological indicators. *Chrysophyte Algae*, Cambridge University Press, Cambridge,
831 pp. 232-268
832 Smolders A.P.J., Lucassen E.C.H.E.T., Roelofs J.G.M. 2002. The isoetid environment biogeochemistry and threats.
833 *Aquat. Bot.*, 73, 325-350
834 Soares A.M.M., Dias J.M.A. 2006. Coastal upwelling and radiocarbon—evidence for temporal fluctuations in
835 ocean reservoir effect off Portugal during the Holocene. *Radiocarbon*, 48 (1), 45-60
836 Sousa A., García-Murillo P., Morales J., García-Barrón L. 2009. Anthropogenic and natural effects on the coastal
837 lagoons in the southwest of Spain (Doñana National Park). *ICES J. Mar. Sci.*, 66, 1508-1514
838 Stevenson A.C. 1984. Studies on the vegetational history of SW Spain III. Palynological investigations at El
839 Asperillo, Huelva. *J. Biogeogr.*, 11, 527-551
840 Stevenson A.C. 1985. Studies in the vegetational history of S.W. Spain. II. Palynological investigations at Laguna
841 de las Madres, Huelva. *J. Biogeogr.*, 12, 243-268
842 Stevenson A.C., Harrison R.J. 1992. Ancient forests in Spain: a model for land use and dry forest management in
843 south-west Spain from 4000 BC to 1900 AD. *Proc. Prehist. Soc.*, 58, 227-247
844 Stevenson A.C., Moore P.D. 1988. Studies in the vegetational history of S.W. Spain. IV. Palynological
845 investigations of a valley mire at El Acebrón, Huelva. *J. Biogeogr.*, 15, 339-361
846 Stockmarr J. 1971. Tablets with spores used in absolute pollen analysis. *Pollen Spores*, 13, 615-621
847 Tanner W.F. 1991. Application of Suite Statistics to Stratigraphy and Sea Level Changes. In J.P.M. Syvitski (Ed.),
848 *Principles, Methods and Applications of Particle Size Analysis*. Cambridge Univ. Press, Cambridge, pp. 283-
849 292

Uzquiano P., Allué E., Antolín F., Burjachs F., Picornel L., Piqué R., Zapata L. 2015. All about yew: on the trail of *Taxus baccata* in southwest Europe by means of integrated palaeobotanical and archaeobotanical studies. *Veg. Hist. Archaeobotany*, 24 (1), 229-247

van Wijk R.J. 1988. Ecological studies on *Potamogeton pectinatus* L. I. General characteristics, biomass production and life cycles under field conditions. *Aquat. Bot.*, 31, 211-258

van Wijk R.J., van Goor E.M.J., Verkley J.A.C. 1988. Ecological studies on *Potamogeton pectinatus* L. II. Autoecological characteristics, with emphasis on salt tolerance, intraspecific variation and isoenzyme patterns. *Aquat. Bot.*, 32, 239-260

Wu L., Dodge L. 2005. Landscape Plant Salt Tolerance Selection Guide for Recycled Water Irrigation. A Special Report for the Elvenia J Slosson Endowment Fund, University of California, Davis (Article. 40)

Yáñez C., Rodríguez Ramírez A., Carrión J.S. 2006. Cambios en la Vegetación de la franja litoral de las marismas de Doñana durante el Holoceno reciente. *An. Biol.*, 28, 85-94

Yll E.I., Zazo C., Goy J.L., Pérez Olbiol R., Pantaleón-Cano J., Civis J., Dabrio C., González A., Borja F., Soler V., Lario J., Luque L., Sierro F., González-Hernández F.M., Lezine A.M., Denèfle M., Roure J.M., Ruiz Zapata B. 2003. Quaternary Palaeoenvironmental Changes in South Spain. *Quaternary Climatic Changes and Environmental Crises in the Mediterranean Region*. Publicaciones de la Universidad de Alcalá, Alcalá de Henares, pp. 201-213

Zazo C., Goy J.L., Somoza L., Dabrio C.J., Belluomini G., Impronta S., Lario J., Bardají T., Silva P.G. 1994. Holocene sequence of sea level fluctuations in relation to climatic trends in the Atlantic-Mediterranean linkage coast. *J. Coast. Res.*, 10 (4), 933-945

Zazo C., Dabrio C., González A., Sierro F., Yll E.I., Goy J.L., Luque L., Panataleón-Cano J., Soler V., Roure J.M., Lario J., Hoyos M., Borja F. 1999. The record of the latter glacial and interglacial periods in the Guadalquivir marshlands (Mari López drilling, S.W. Spain). *Geogaceta*, 26, 119-122

Zazo C., Dabrio C.J., Goy J.L., Lario J., Cabero A., Silva P.G., Bardají T., Mercier N., Borja F., Roquero E. 2008. The coastal archives of the last 15 ka. In the Atlantic-Mediterranean Spanish linkage area: sea level and climate change. *Quat. Int.*, 181, 72-87

Zunzunegui M. 1997. *Respuestas de la Vegetación a Ambientes Fluctuantes en el Parque Nacional de Doñana*. PhD Thesis, Universidad de Sevilla

880 **Table and Figure captions**

881

882 **Table 1**. LuCA Radiocarbon dates.

laboratory code[a]	Depth (cm)	Thickness (cm)	Calibration curve[b]	Radiocarbon age (yr BP)	Calibrated age ranges[b](yr cal BP)
ETH-57403	42	2	IntCal13.14C	5702 ± 34	6407–6566
ETH-57405	205	2	IntCal13.14C	7015 ± 36	7783–7938
ETH-57405c	280	2	IntCal13.14C	12,312 ± 46	12,100–12,700
ETH-57407	476	2	Marine13	7364 ± 37	7644–8011
Poz-55,367	615	4	Marine13	7830 ± 40	8105–8460
Poz-55,368	711	4	Marine13	9180 ± 50	9615–10,319

883 [a] Reimer et al. (2013).

884 [b] 95% confidence intervals.

885 [c] Excluded from the age-depth model for being considered too old.

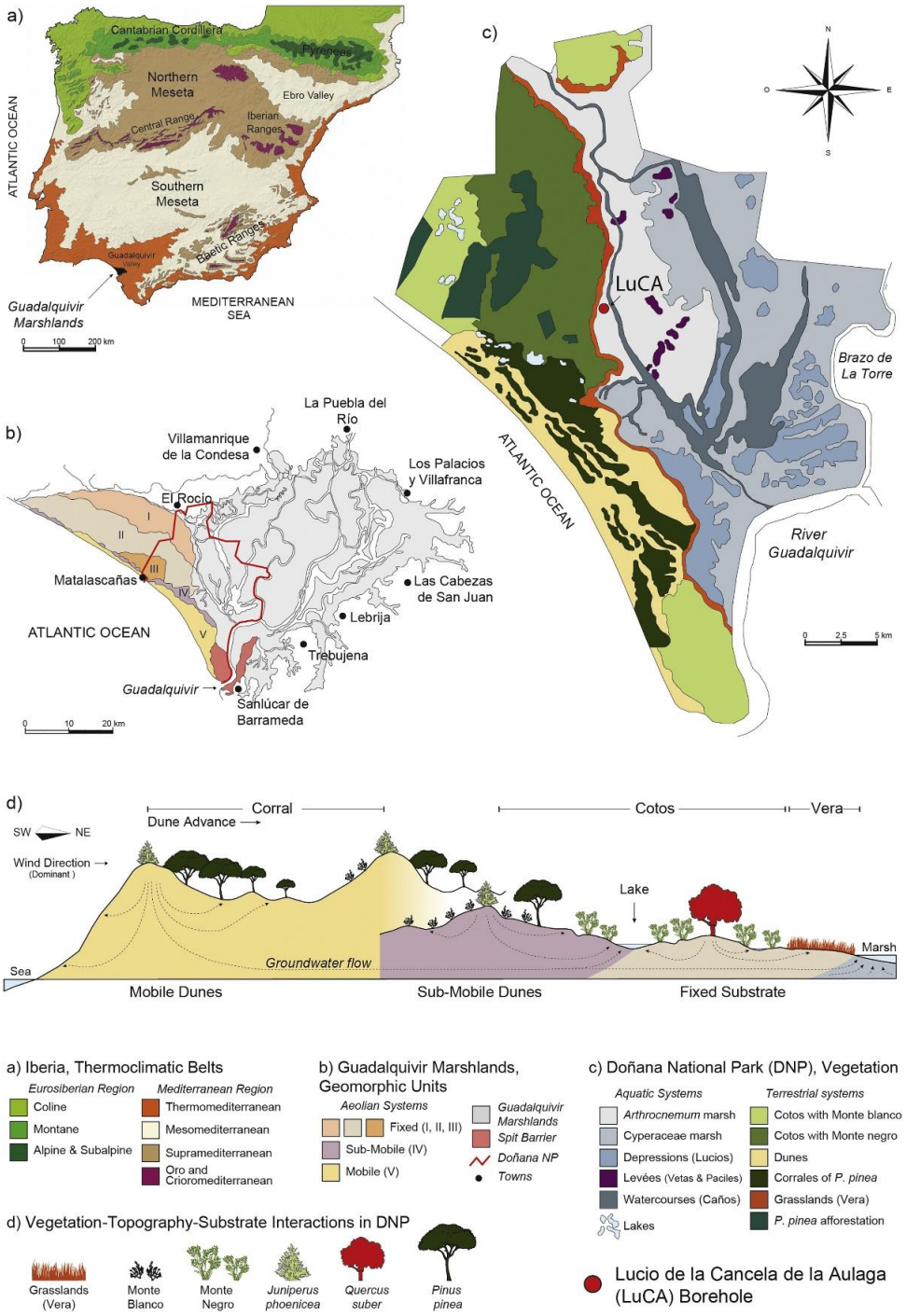

Figure 1. Study area. (a) Iberia, thermoclimatic belts (modified from Manzano et al., 2017). Note that the region concerning this work is marked in the SW in black. (b) Guadalquivir Marshlands and geomorphic units in the Doñana National Park area (limited in red) and surroundings (Modified from López Albacete, 2009 and Rodríguez Ramírez, 1997). (c) Main Doñana National Park (DNP) systems (aquatics and terrestrial) and associated vegetation therein (modified from Zunzunegui, 1997 and own data). The study site is marked with a red dot and labelled. (d) Vegetation-Topography-Substrate Interactions SW-NE transect in DNP (modified from López Albacete, 2009, Manzano et al., 2013, Rivas Martínez et al., 1980 and own data).

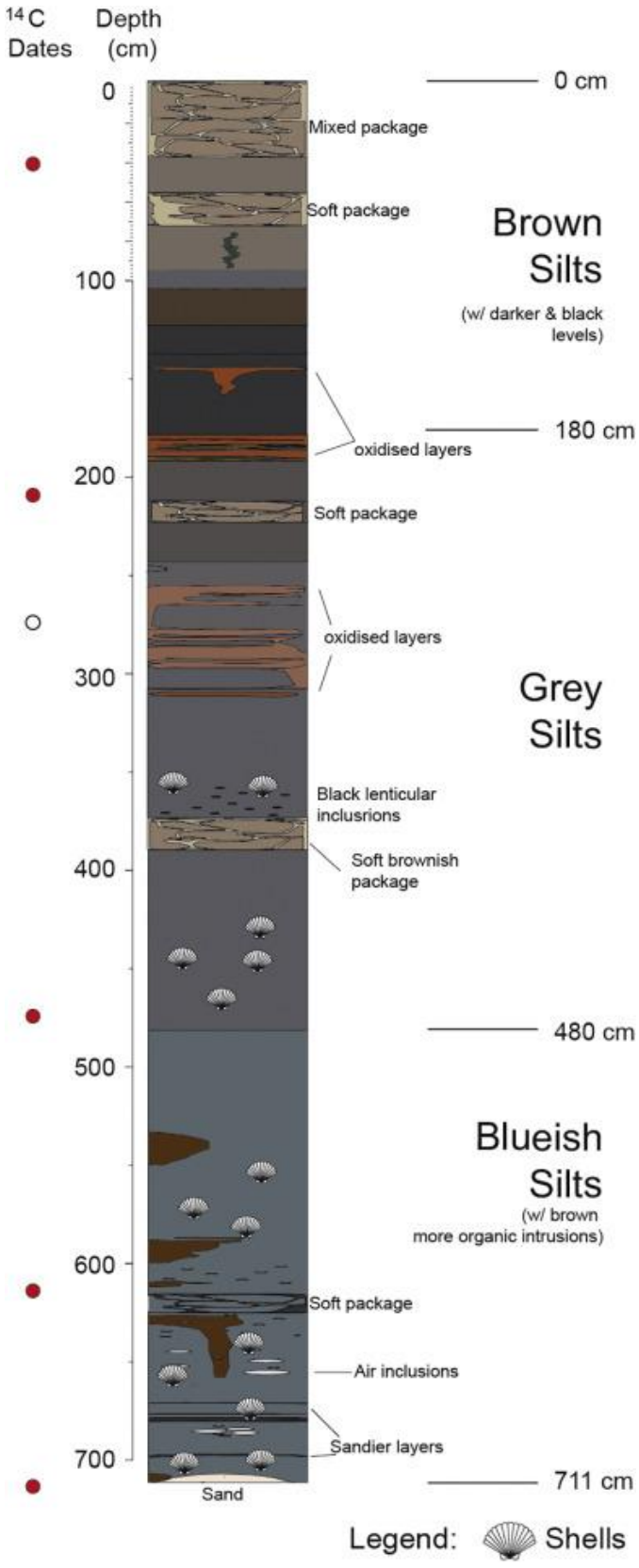

Figure 2. Schematic representation of the LuCA sedimentary core showing the main facies stratigraphy and the location of the radiocarbon dates along the sequence. Filled dots represent the radiocarbon dates included in the age-depth model, the blank dot the discarded date.

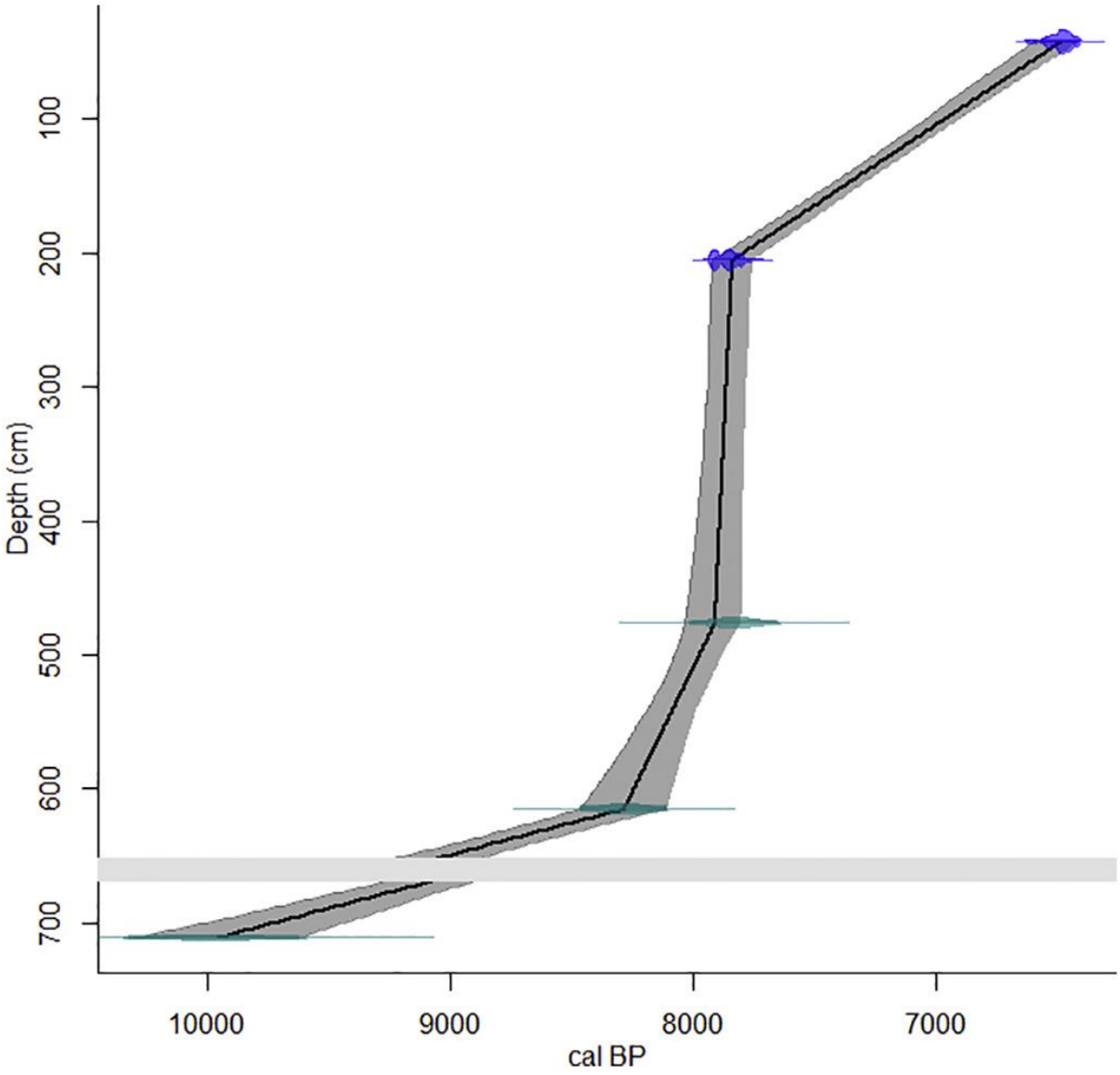

899

900 **Figure 3.** Age-depth model of the LuCA sedimentary core. Dark blue radiocarbon dates are calibrated
901 with the IntCal13.14C terrestrial calibration curve, while light blue dates are calibrated with the
902 Marine13 curve. The horizontal grey bar represents the excised slump (668–654 cm depth, see
903 Discussion for interpretation).

904

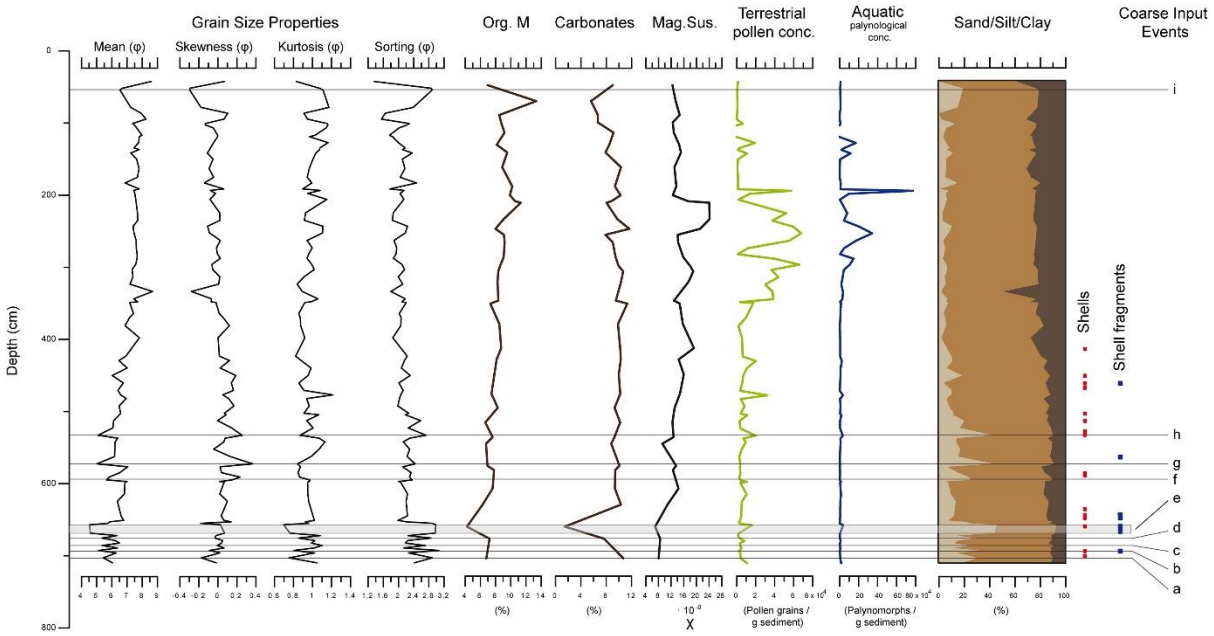

Figure 4. Sedimentological record of the LuCA sequence plotted in depth including, from left to right: grain size analysis distribution properties, organic matter (org. M) and carbonate content, magnetic susceptibility (Mag. Sus), terrestrial and aquatic pollen concentration, sand/silt/clay sedimentology log, shell and shell fragment presence and coarse input events. The lettered levels (a–i), identified by dashed lines, indicate coarse input events.

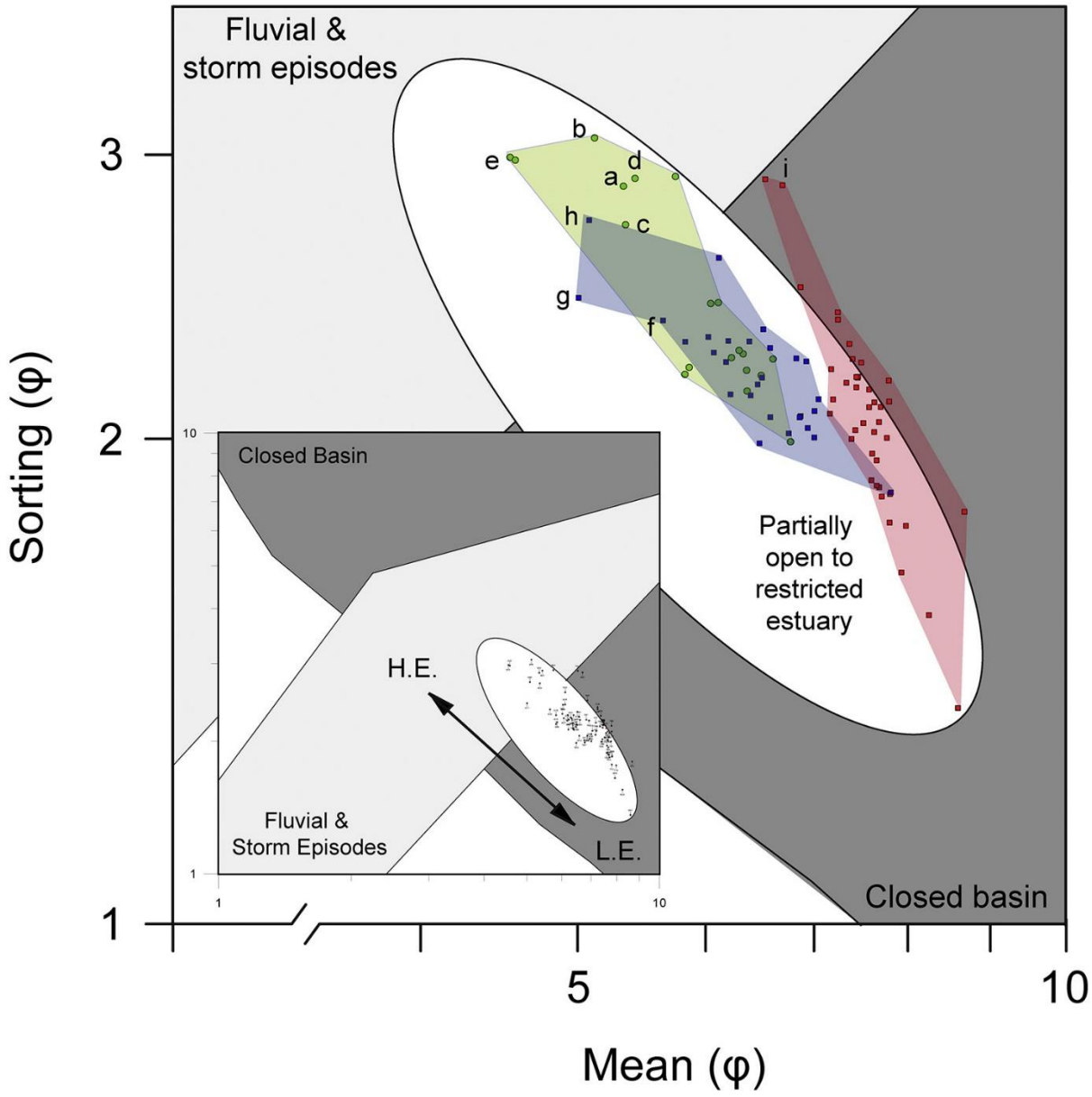

912

913 **Figure 5.** Suite analysis. Mean grain size (ϕ) vs. sorting (ϕ) of sediments from the LuCA sequence
914 (diagram template modified from Tanner, 1991), segregating samples between partially restricted-
915 open or closed estuary depositional conditions. Displacement along the high energy (H.E)-low energy
916 (L.E.) diagonal axis, as oriented in the miniature, indicate depositional energy. Filled polygons group
917 chronologically the LuCA samples; green (9.9–8.2 cal. kyr BP), blue (8.2-7-8 cal. kyr BP), red (7.8–6.4
918 cal. kyr BP).

919

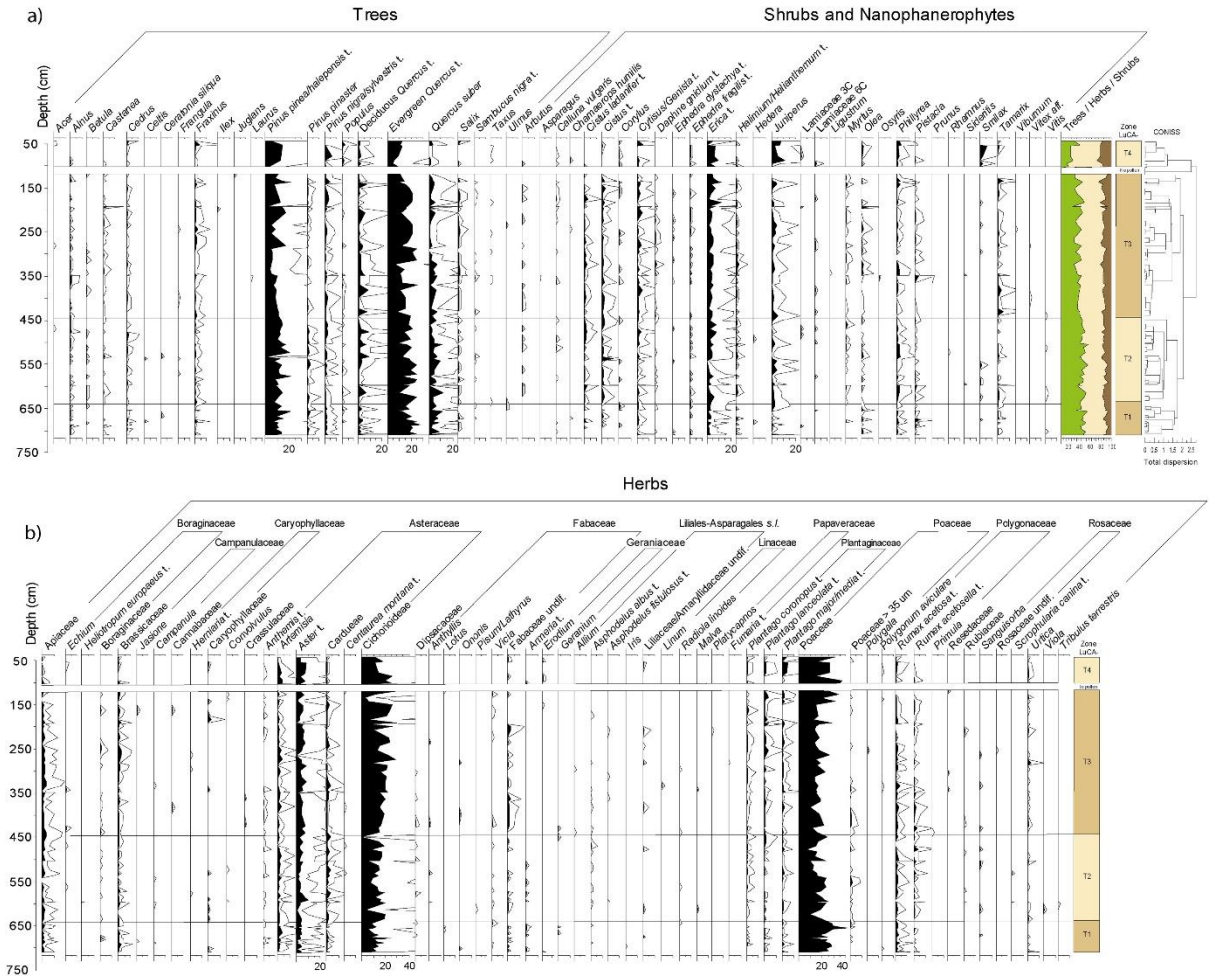

920

921 **Figure 6.** LuCA pollen diagram represented in depth (cm): a) trees, shrubs and nanophanerophytes; b)
922 herbs; c) ferns, bryophytes and fungi; d) helophytes and macrophytes; and e) algae, protozoa and
923 invertebrates. Exaggerated values (× 5) have been plotted in white curves.

924

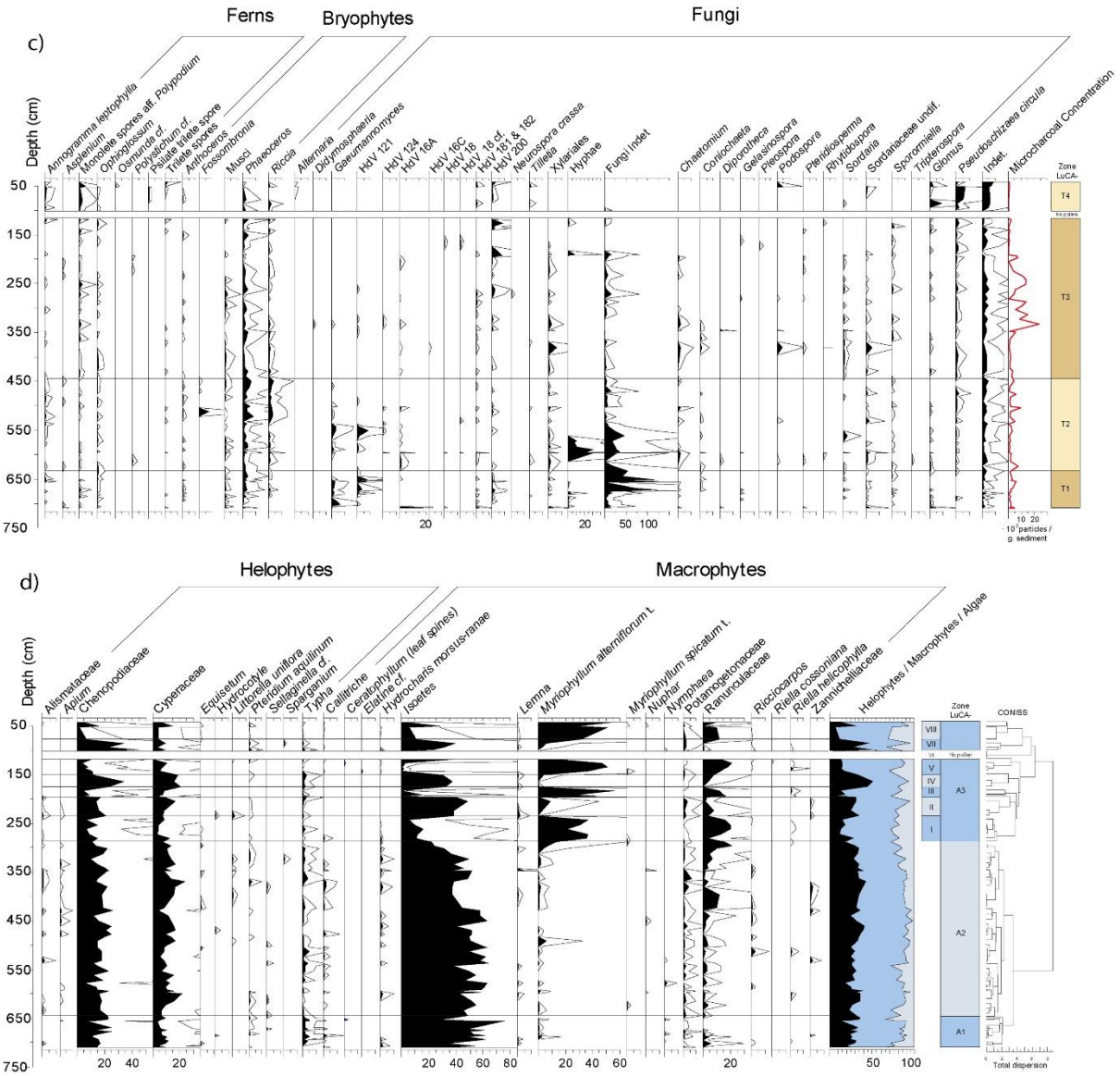

925

926 **Figure 6.** LuCA pollen diagram represented in depth (cm): a) trees, shrubs and nanophanerophytes; b)
927 herbs; c) ferns, bryophytes and fungi; d) helophytes and macrophytes; and e) algae, protozoa and
928 invertebrates. Exaggerated values (× 5) have been plotted in white curves.

929

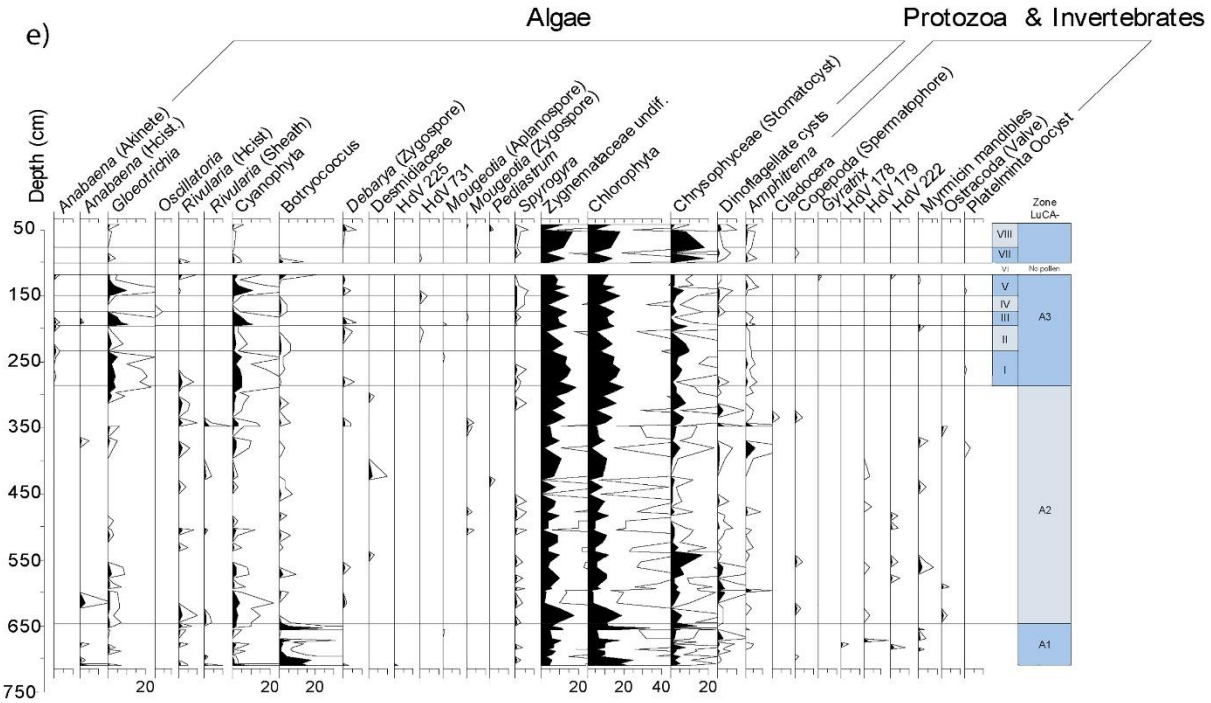

930

931 **Figure 6.** LuCA pollen diagram represented in depth (cm): a) trees, shrubs and nanophanerophytes; b)
932 herbs; c) ferns, bryophytes and fungi; d) helophytes and macrophytes; and e) algae, protozoa and
933 invertebrates. Exaggerated values (× 5) have been plotted in white curves.

934

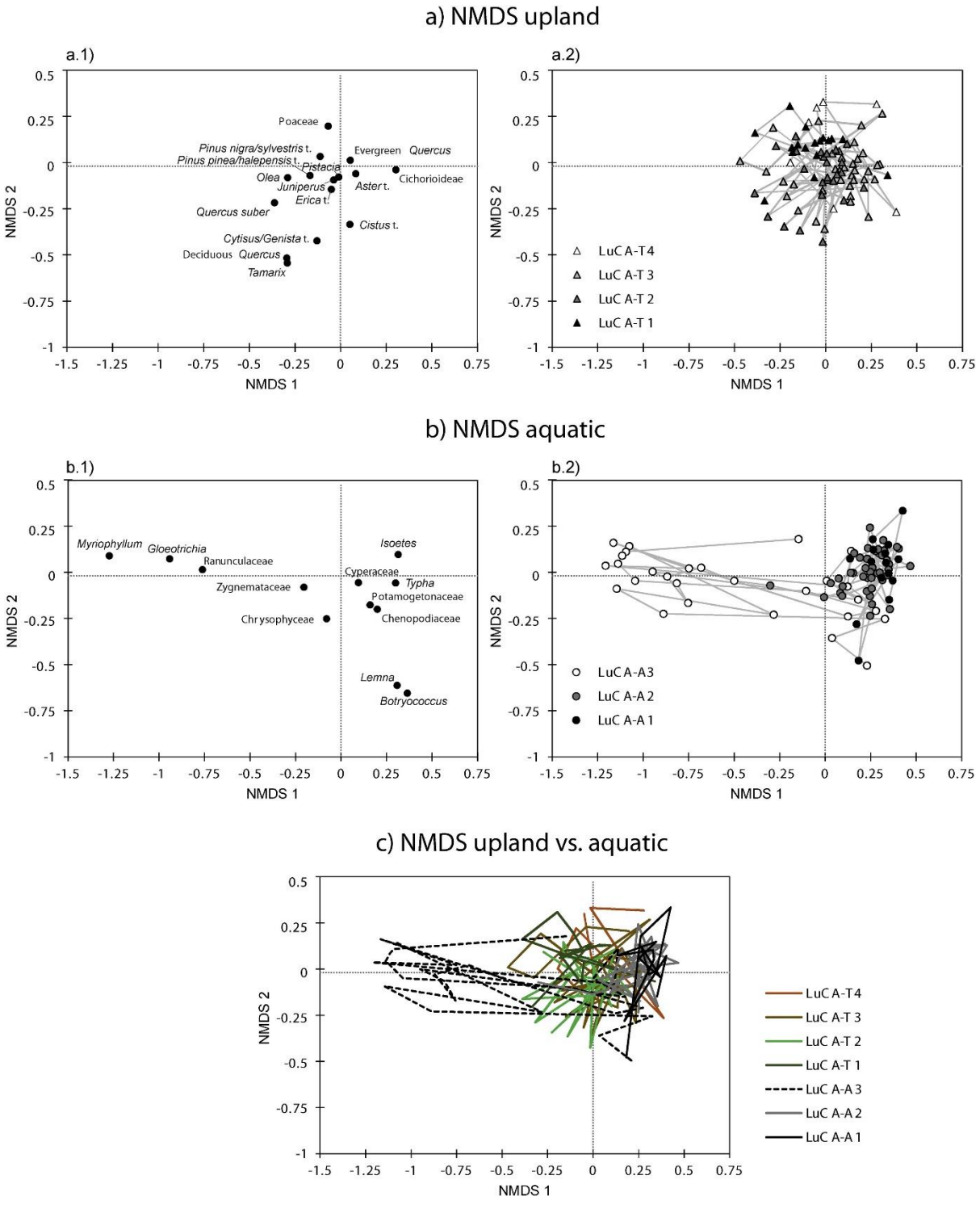

935

936 **Figure 7.** NMDS ordination of the LuCA pollen data. a) NMDS ordination of the upland component;
937 a.1) NMDS upland taxa loadings; a.2) NMDS upland sample loadings. b) NMDS ordination of the
938 aquatic component; b.1) NMDS aquatic taxa loadings; b.2) NMDS aquatic sample loadings. c)
939 Comparison of the upland and aquatic NMDS ordinations.

940

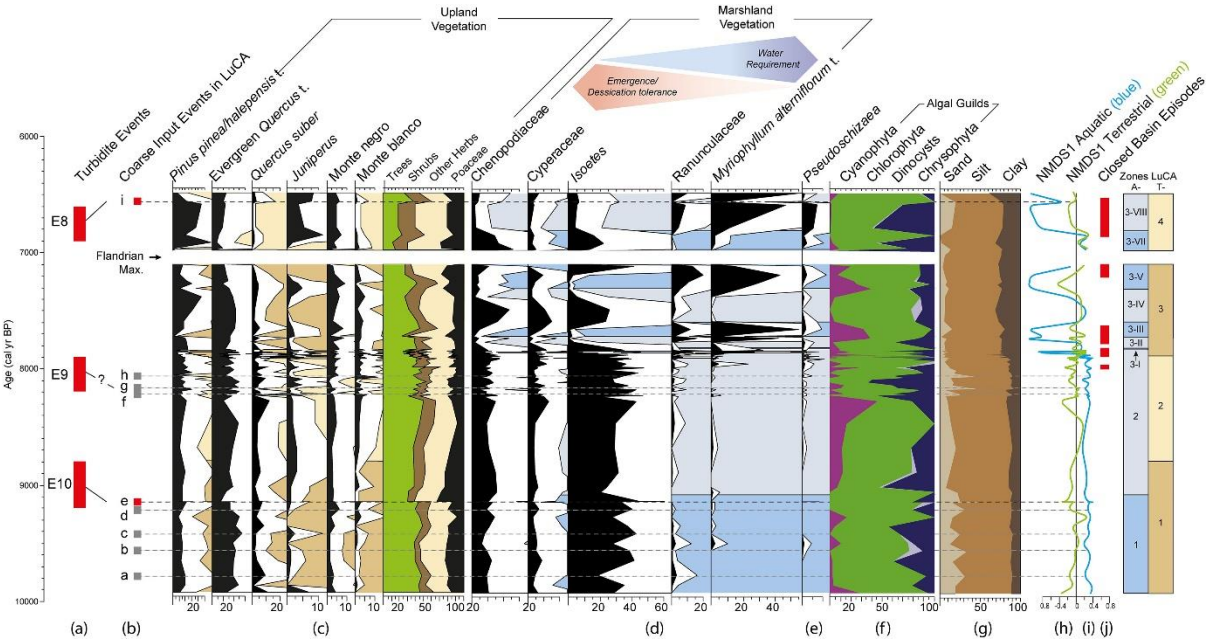

941

942 **Figure 8.** Chronology of the environmental changes detected in Doñana after the study of the LuCA
943 palaeoecological sequence. a) Turbidite events (Gràcia et al., 2010); b) LuCA coarse input events; c)
944 selected upland vegetation taxa pollen diagram; Monte negro includes the sum of the locally edapho-
945 higrophilous shrubs and nanophanerophytes (*Arbutus*, *Calluna vulgaris*, *Cystisus/Genista* type, *Erica*
946 type, *Hedera*, *Ligustrum*, *Myrtus*, *Olea*, *Phillyrea*, *Pistacia*, *Prunus*, *Rhamnus*, *Smilax* and *Viburnum*).
947 Monte blanco includes the sum of the locally edapho-xerophilous taxa (*Asparagus*, *Cistus* type, *C.*
948 *ladanifer* type, *Chamerops humilis*, *Daphne gnidium* type, *Ephedra dystachya* type, *E. fragilis* type,
949 *Halimium/Helianthemum* type, Lamiaceae 3C and 6C, and *Sideritis*). d) Selected marshland vegetation
950 taxa palynological diagram, indicating taxa water requirements; e) *Pseudoschizaea circula*; f) Algal
951 guild proportions; g) LuCA sand, silt and clay sedimentology log; h) NMDS1 axis for terrestrial taxa
952 (green); i) NMDS1 axis for aquatic taxa (blue); j) LuCA closed basin episodes.

953

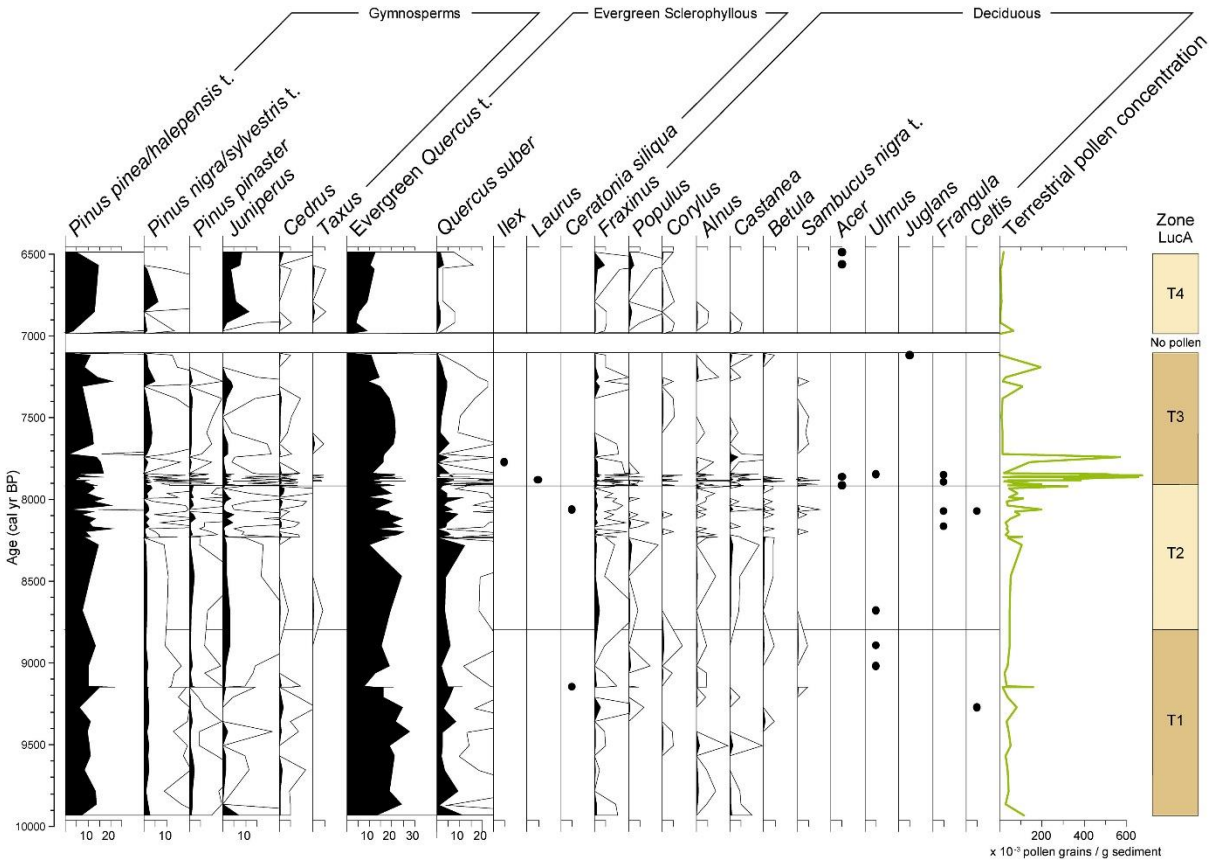

954

955 **Figure 9.** Selected taxa of biogeographical relevance from the LuCA palynological record.